

To Anonymous Referee #2,

The authors sincerely appreciate your review and valuable comments.

*Suggested title change: “Comparison of Vaisala RS41 and RS92 radiosondes launched over the oceans from the Arctic to the Tropics”*

*Line 18: suggested rewording, “RS41-SGP, sonde version with pressure sensor, : : :”*

*Line 29-30: suggested change, “discrepancies presumably caused by the “wet-bulbing” effect on the RS92 sonde and the stagnation : : :”*

*Line 40: suggested rewording, “are operationally conducted : : :”*

*Line 43: suggested rewording, “ with helium or hydrogen gas.”*

*Line 50: suggested rewording, “Efforts to improve the quality of : : :”*

➔ We corrected these five sentences and the title in the revised manuscript (Line 1-3, 19, 31-32, 42, 45, 52-53).

*Line 53: suggest you add reference to the end of this sentence to (Wang et al. 2013)*

*Reference is: Wang, J., L. Zhang, A. Dai, F. Immler, M. Sommer, and H. Vömel, 2013: Radiation dry bias correction of Vaisala RS92 humidity data and its impacts on historical radiosonde data. J. Atmos. Oceanic Technol., 30, no. 2, 197-214.*

➔ We added this reference to the manuscript (Line 56).

*Line 95-98: Is this special note really needed? I would suggest you eliminate this but then say: “All RS92 sonde data used in this study were processed with DigiCORA software v3.64 which includes humidity corrections for solar radiation dry bias and timelag errors due to the slow response of the humidity sensors (Dirksen et al., 2014).” Reference is: Dirksen, R. J., M. Sommer, F. J. Immler, D. F. Hurst, R. Kivi, and H. Vömel, 2014: Reference quality upper-air measurements: GRUAN data processing for the Vaisala RS92 radiosonde. Atmos. Meas. Tech., 7, 4463-4490.*

➔ This part was deleted before the manuscript was published as a discussion paper in AMTD. (indicated by Anonymous Referee #1)

*Line 128: Suggest you start paragraph with a introductory sentence something like: “A number of issues were addressed in post-processing the sounding data.”*

➔ We added this sentence to the beginning of the paragraph (Line 134).

*Line 129: Suggested rewording: “the radiosondes oscillated vertically about the 0\_C level likely due to icing on the balloon, and hence only : : :”*

➔ We corrected this sentence (Line 135-137).

*Line 152 and following: Is it possible to compute pressure from the RS41 GPS height data similar to what is done with RS41 SG sondes, that is sondes without a pressure sensors? Would this GPS computed pressure lead to an improved comparison with pressure from the RS92 sondes as found in Jensen 2016. If there is an improved comparison using GPS computed pressure, this could be a useful recommendation for future use.*

➔ We checked the GPS-derived pressure of the RS41 radiosondes (it seems that we usually cannot obtain it by the normal use of the software). New Figure 4 shows the difference between the RS92 pressure and the RS41 GPS-derived one. The use of the GPS-derived pressure reduces the bias by approximately 0.2 hPa above an altitude of 15 km, but there is still a bias of 0.4 hPa or more at most of altitudes. The median of the difference in Fig.4 is almost the same as in Fig.3a around an altitude of 5 km. The GPS does not essentially improve the pressure bias. This description was added to section 3.1 and conclusions (Line 170-176).

*Following section 3.1: It would be useful to see how these pressure difference translate into geopotential height differences. I would suggest adding another panel to Fig. 3 where you show the height differences.*

➔ We added a panel to show the difference in height to Fig.3. New Figure 3b shows that the height difference increased as the radiosondes rose higher: The median of the RS41 height was greater than that of the RS92 by approximately 35 m at an altitude of 15 km, and 100 m at 22 km. These height differences correspond to the differences of pressure. This description was added to section 3.1 and conclusions (Line 166-169, 338-340).

*Line 200: In discussing Fig. 6a and the differences in the T and RH profiles between the sondes, can you speculate which sonde would be less prone to errors due to poor ventilation? Why?*

➔ We speculate that the RS92 temperature and humidity would be closer to true values in this case because they changed more quickly than the RS41 ones, which suggests the better ventilation of the RS92 radiosonde.

*Line 201 and following regarding Figs. 6b and 6c: The large temperature differences seen at low-levels would likely results in significant differences in CAPE and CIN. It would be informative to list*

*these CAPE and CIN differences as additional motivation for better understanding this issue.*

- ➔ We added the values of CAPE, CIN, and PW to Table 2, and new Table 4 lists their statistics. The large temperature differences near the sea surface shown in Fig.6b-c caused large discrepancies in CAPE (the difference in CIN was small). We added this description to the manuscript (Line 130-133, 222-224).

*Line 217: Are the noisier wind speed data in this study compared to Jensen's related to the observations being taken on a ship and hence ship motion? Also is there an explanation for the large mean wind differences above 27 km in Figs 3d and 3e?*

- ➔ Ship motion never affects the measurement of radiosondes because the radiosondes is not on the ship after the launch and the motion of the receiving system will not make any noise.

*Line 241: suggested rewording: "bias was generally absent from later observations processed with V3.64 software (Ciesielski : : :).*

- ➔ We corrected this sentence (Line 261-263).

*Line 251 and following: It seems you are assuming that the moisture biases between the sondes are always related to issues with the RS92 sonde. Is there any independent confirmation you can provide (GPS or microwave PW estimates or preferably snow white chilled mirror soundings) that in fact show the RS92 sondes having the poorer performance. Can you discount the fact that the RS41 doesn't have slight moist bias? Regarding this, it would be instructive if you could produce a similar diagram to Fig. 18 in Jensen et al (2016) which showed PW estimates from both the RS41, RS92 and some independent estimate and then discuss the findings. Jensen et al. (2016) claim their comparison between sonde and MWR PW may have been affected by spatial moisture gradients near the launch site. Spatial moisture gradients should not be as much of an issue for your oceanic soundings, such that a PW comparison between sondes and some independent estimate could be quite instructive. Finally, if you are including PW estimates from the RS41 and RS92 sondes, it would be useful to also see CAPE and CIN differences (either in tabular or graphical form) for each sonde launch.*

- ➔ We don't believe the biases are always due to RS92's fault only. We have no independent evidence to prove that the RS92 accuracy is worse than the RS41, and recognize the possibility that the RS41 data also might have had a bias. We added this explanation to the revised manuscript (Line 290-296). (Another researchers who participated in only the MR15-04 cruise attempted to measure PW by using a shipborne GPS, but we cannot use their GPS-derived PW at present. They found a mistake in their data processing and their data are still being reprocessed. In any case,

the shipborne GPS-derived PW is expected to have an RMS error of about 3.0 mm compared with radiosonde PW (Fujita et al. 2008) and this will not be a decisive factor to judge which radiosonde is better.) Certainly the comparison between the GPS-derived PW and radiosonde PW is an interesting topic, but this is beyond the scope of the research on the difference between the two types of radiosondes.

New Table 4 lists the statistics of CAPE, CIN, and PW, and we mentioned how the differences between the RS41 and RS92 affected the calculations of CAPE, CIN, and PW (Line 273-286, and new Fig.10).

*Line 251: You note that there is a residual day-time dry bias in the RS92 data but there also appears to be a night-time dry bias (at least between 3-13 km). This nighttime difference is certainly not caused by differences in the radiation correction schemes in the sonde software. Please comment?*

➔ We agree with you on this point. The RS41 humidity may have a slight moist bias that is unrelated to the radiation correction scheme below an altitude of 13 km. We added this indication to the revised manuscript (Line 292-294).

*Line 254: “proposed by Nuret et al. (2008) : : :” Reference is Nuret, M., J.-P. Lafore, F. Guichard, J.-L. Redelsperger, O. Bock, A. Agusti-Panareda, and J.-B. N’Gamini, 2008. Correction of humidity bias for Vaisala RS80-A sondes during the AMMA 2006 observing period. J. Atmos. Oceanic Technol., 25, 2152-2158. It would be useful to include local time and precipitable water (PW) in table 2. The PW values would allow one to better gauge the range of moisture conditions the sondes were launched in. If you show PW values in a separate figure (see comments above) then putting them in table 2 would not be necessary. If more room is needed, the lat/lon values can be truncated to 1 or 2 decimal places.*

➔ Nuret et al. (2008) was cited in the revised manuscript (Line 298). Local time and PW have been added to Table 2. PW values are also shown in new Fig.10.

*Figure 3, panels (b) and (c) appear to be switched in this figure caption. However you may want to switch these panels to make them consistent with Jensen’s Fig. 8.*

➔ The caption of Fig.3 was wrong. We corrected it.

*Minor grammatical comments:*

*Line 26: suggested rewording, “4.5 km, suggesting that there : : :”*

*Line 37: “further studies on the causes : : :”*

*Line 143: “To facilitate comparison : : :”*

*Line 267: “range of temperatures and relative humidities”*

*Line 269: “was largest : : .”*

*Tabel 2: “Wind dir.”*

➔ We corrected them (Line 27, 39, 151, 312).

To Anonymous Referee #3,

The authors sincerely appreciate your review and valuable comments.

*My only question to the authors is the following: To what extent can the differences between the results obtained for pressure in this study compared to previous studies be explained by the fact that this study did not use GPS-measured height to derive pressure?*

*Can you add a sentence or two on this topic to Section 3.1 or to the discussion section? Do the measurements collected allow you to test what the differences would be if pressure were derived from GPS-measured height?*

➔ We checked the GPS-derived pressure of the RS41 radiosondes (it seems that we usually cannot obtain it by the normal use of the software). New Figure 4 shows the difference between the RS92 pressure and the RS41 GPS-derived one. This figure exactly corresponds to Fig.8a of Jensen et al. (2016). The use of the GPS-derived pressure reduces the bias by approximately 0.2 hPa above an altitude of 15 km, but there is still a bias of 0.4 hPa or more at most of altitudes. The median of the difference in Fig.4 is almost the same as in Fig.3a around an altitude of 5 km. The GPS does not essentially improve the pressure bias. This description was added to section 3.1 and conclusions (Line 170-176).

To Anonymous Referee #1,

The authors sincerely appreciate your review and valuable comments. We posted a revised manuscript on 25 April, and further revised the manuscript, considering your comments.

*1. Lines 101-103: Even though you did not use the GPS-derived pressure and height measurements, I think it would be good in this study to mention what the RS41 GPS-derived pressure and height measurements are. Comparing these measurements to the in-situ measured pressure would strengthen the claim that the pressure bias is real – considering the GPS-derived pressure and in-situ measured pressure are literally on the same instrument. It would also be good to make sure that the GPS-derived pressure and height measurements are the same between the RS41 and RS92.*

➔ We checked the GPS-derived pressure of the RS41 radiosondes. New Figure 4 in the revised manuscript shows the difference between the RS92 pressure and the RS41 GPS-derived one. The use of the GPS-derived pressure reduces the bias by approximately 0.2 hPa above an altitude of 15 km, but there is still a bias of 0.4 hPa or more at most of altitudes. The median of the difference in Fig.4 is almost the same as in Fig.3a around an altitude of 5 km. This means that the GPS does not essentially improve the pressure bias, and the reason for the pressure bias is still unknown. We also added a panel to show the difference in height to Fig.3. Figure 3b shows that the height difference increased as the radiosondes rose higher: The median of the RS41 height was greater than that of the RS92 by approximately 35 m at an altitude of 15 km, and 100 m at 22 km. These height differences correspond to the differences of pressure. These descriptions were added to section 3.1 and conclusions (Line 166-176, 338-340).

*2. Figure 2, and general comment about the pressure bias: Compared to Jensen et al., 2016, the twin soundings are literally attached together. I think the pressure bias may have inadvertently been caused by drag created by the balloon above it. To explain further, you noted that the pressure bias was larger above 4.5 km and was especially noticeable during the day. During ascent, the balloon itself expands, thus creating a larger object displacing the air above it. Similar to how a falling raindrop has a local high pressure at the base of the drop and a local negative pressure at the “tail” of the drop, perhaps the balloon itself is creating a local minimum pressure tendency below the balloon (i.e. in the same area the twin sondes are located)? I included a sketch on the last page to help explain this. GPS measurements, of course, should be unaffected by this. If the pressure bias is indeed created by drag, then that also adds some credence to using a bar (like in Jensen et al., 2016) to horizontally hang the twin sensors, as opposed to attaching them together by tape – the sondes hung on the edges of the bar would be further away from the area of maximum local negative pressure tendency induced by the drag. It would also be worthwhile to mention in your conclusions that a comparison of the in-situ silicon sensor vs. the GPS-derived pressure on the same balloon should be done – this could either confirm or eliminate the possibility of air drag affecting the in-situ pressure measurement. With this idea in mind, it is very well*

*possible that the pressure sensor is affected by solar heating as well, especially since pressure is measured by a capacitive element.*

➔ The difference between the RS41 sensor-measured pressure and GPS-derived one (see Fig.3a and Fig.4 in the revised manuscript) indicates that the stagnation below the balloon might have slightly contributed to lowering the sensor-measured pressure. However, this was not the main reason for the pressure bias between the RS41 and RS92, as we mentioned above. We used a string of 55m originally supplied to the RS41 radiosonde and our twin-radiosonde flight was the same as the standard RS41 flight, except for that an additional radiosonde was attached and the balloon was relatively large (350g). We think that this factor is inessential in the pressure bias.

*3. Lines 236-238: The reason the RS92 solar radiative dry bias was absent in the two papers you cited is because they used the relative humidity correction scheme according to Wang et al. (2013; citation provided below). Please include this citation here, and clarify this sentence by mentioning that the absent dry-bias is because this RH correction scheme was implemented.*

*Wang, J., Zhang, L., Dai, A., Immler, F., Sommer, M., and Vömel, H., 2013: Radiation dry bias correction of Vaisala RS92 humidity data and its impacts on historical radiosonde data. Journal of Atmospheric and Oceanic Technology, 30, 197-214.*

➔ We added your indication to this sentence (Line 262-263).

*4. Lines 226 and 242: In addition to the Wang et al. (2013) and Yu et al. (2015) studies already mentioned above or cited already, you may want to consider including these additional citations, as they all expand upon the solar radiative dry bias at high altitudes and discuss various approaches to correcting (and independently validating) the solar radiative induced RH dry bias. The Miloshevich et al. (2009) paper has a very thorough discussion in Section 4.2 on nighttime RH measurements and may be relevant to your discussion on Figure 7. All of these studies also use precipitable water vapor (PWV) as a reference measurement, and it would be good to include measurements of PWV (perhaps from GPS or microwave radiometer retrievals) to show how much poorer the RS92 RH measurements are compared to the RS41, if its even significant at all.*

*Miloshevich, L. M., H. Vömel, D. N. Whiteman, and T. Leblanc, 2009: Accuracy assessment and correction of Vaisala RS92 radiosonde water vapor measurements, J. Geophys. Res., 114, D11305, doi:10.1029/2008JD011565.*

*Dzambo, A. M., Turner, D. D., and Mlawer, E. J., 2016: Evaluation of two Vaisala RS92 radiosonde solar radiative dry bias correction algorithms, Atmos. Meas. Tech., 9, 1613-1626, doi:10.5194/amt-9-1613-2016, 2016.*

*Moradi, I., B. Soden, R. Ferraro, P. Arkin, and H. Vömel, 2013: Assessing the quality of humidity measurements from global operational radiosonde sensors, J. Geophys. Res. Atmos., 118, 8040–8053 doi:10.1002/jgrd.50589.*



➔ We showed analyses of CAPE, CIN, and PW, and added a figure of the ratio of RS41 PW to RS92 PW as a function of solar altitude angle in the new revised one (new Fig.10). Similar to Fig.4a of Miloshevich et al. (2009), the ratio was dependent on solar altitude angle. This description was added to section 4.1 (Line 273-286).

It seems that the nighttime moist bias of RS92 at the altitude of 15-20 km (Fig.8c) might have been partly ascribed to the time-lag error (Fig.11c in Miloshevich et al. 2009), but I'm not confident of it since the time-lag error must have been corrected in the latest software.

*5. Lines 243-246: The reason the values in your Figure 8 agree better than Figure 6 in Vömel et al. (2007) is likely because Figure 6 compares Vaisala RS92 data (before DigiCora v. 3.64 data) to cryogenic frost point hygrometer data, which is widely regarded as one of the best reference instruments in developing RH correction algorithms. In your Figure 8, you compare RS92 DigiCora v. 3.64 data to RS41 data, both of which are much better at measuring relative humidity. You should note, perhaps at the end of this sentence, that the values in Fig. 8 are less than Fig. 6 in Vömel et al. (2007) because the RS92 DigiCora v. 3.64 RH data and RS41 RH data are already inherently better.*

➔ We added your indication to this sentence (Line 271-272).

*Technical Comments:*

*1. Line 165: Change “: : : radiosonde tended to record a higher mean relative humidity than the: : :” to “: : : radiosonde recorded a higher mean relative humidity relative to the: : :”*

➔ We corrected this sentence (Line 186-187).

# Comparison of Vaisala radiosondes RS41 and RS92 ~~in-~~ launched over the oceans ~~ranging~~ from the Arctic to the Ttropics

Yoshimi Kawai<sup>1</sup>, Masaki Katsumata<sup>1</sup>, Kazuhiro Oshima<sup>2</sup>, Masatake E. Hori<sup>2</sup>, and Jun  
Inoue<sup>3</sup>

<sup>1</sup>Research and Development Center for Global Change, Japan Agency for Marine–Earth  
Science and Technology, Yokosuka 237-0061, Japan

<sup>2</sup>Institute of Arctic Climate and Environment Research, Japan Agency for Marine–Earth  
Science and Technology, Yokosuka 237-0061, Japan

<sup>3</sup>Arctic Environment Research Center, National Institute of Polar Research, Tachikawa  
190-8518, Japan

*Correspondence to:* Yoshimi Kawai (ykawai@jamstec.go.jp)

**Abstract.** To assess the differences between the RS92 radiosonde and its improved  
counterpart, the Vaisala RS41-SGP, radiosonde version with ~~radiosonde that has a~~  
pressure sensor, 36 twin-radiosonde launches were made over the Arctic Ocean, Bering  
Sea, northwestern Pacific Ocean, and the tropical Indian Ocean during two cruises of the

22 R/V *Mirai* in 2015. The biases, standard deviations, and root mean squares (RMSs) of the  
23 differences between the RS41 and RS92 data over all flights and altitudes were smaller  
24 than the nominal combined uncertainties of the RS41, except that the RMS of the  
25 differences of pressure above 100 hPa exceeded 0.6 hPa. A comparison between daytime  
26 and nighttime flights in the tropics revealed that the pressure difference was systematically  
27 larger during the day than at night above an altitude of 4.5 km, ~~the suggesting~~ngon being that  
28 there was some effect of solar heating on the pressure measurements, but the exact  
29 reason is unclear. The agreement between the RS41 and RS92 temperature  
30 measurements was better than the combined uncertainties. However, there were some  
31 noteworthy discrepancies ~~that were~~ presumably caused by the “wet-bulbing” effect on the  
32 RS92 radiosonde and the stagnation of the balloon. Although the median of the relative  
33 humidity differences was only a little more than 2 % of the relative humidity at all altitudes,  
34 the relative humidity of the RS92 was much lower than that of the RS41 at altitudes of about  
35 17 km in the tropics. This dry bias might have been caused by the incomplete solar  
36 radiation correction of the RS92, and a correction table for the daytime RS92 humidity was  
37 calculated. This study showed that the RS41 measurements were consistent with the  
38 specifications of the manufacturer in most cases over both the tropical and polar oceans.  
39 However, further studies ~~of~~on the causes of the discrepancies are needed.

40

## 41 1 Introduction

42 Radiosonde observations are operationally ~~regularly~~ conducted twice a day at about 800  
43 sites throughout the world. Radiosondes measure temperature, humidity, wind velocities,  
44 and pressure (or height) in the troposphere and stratosphere. They ascend through the  
45 atmosphere attached to balloons filled with helium or hydrogen gas. The data are sent to  
46 the global telecommunication system and are used for data assimilation in real-time  
47 operational weather forecast systems, atmospheric reanalyses, and climate models. In situ  
48 aerological observations are also indispensable for validating satellite-derived  
49 meteorological data (e.g. Fujita et al., 2008), for assessing long-term trends in the upper  
50 atmosphere (e.g. Thorne et al., 2005; Maturilli and Kayser, 2016), and for other  
51 meteorological research, including assimilation experiments and air-sea interaction studies  
52 (e.g. Inoue et al., 2013; 2015; Kawai et al., 2014). Efforts to improve the quality ~~enhance the~~  
53 ~~reliability~~ of radiosonde data have continued to the present time (e.g. Ciesielski et al., 2014;  
54 Bodeker et al., 2016). One consequence of the technological advancements has been the  
55 need to account for accuracy differences following radiosonde upgrades in the long-term  
56 continuous datasets (Wang et al., 2013).

57 The model RS92 radiosonde manufactured by Vaisala Ltd., which was first introduced  
58 in 2003, has been used throughout the world, and it is now being replaced with a successor  
59 model, the RS41 (Table 1). To clarify the differences between the RS41 and RS92  
60 radiosondes, intercomparison experiments have already been carried out at several sites

61 on land from high latitudes to the tropics (Möhl, 2014; Jauhiainen et al., 2014; Jensen et al.,  
62 2016). Jauhiainen et al. (2014) have reported results of comparisons in several countries,  
63 including Finland, the United Kingdom, the Czech Republic, and Malaysia. They reported  
64 that the RS41 radiosonde was a consistent improvement over the RS92 in terms of  
65 reproducibility with respect to temperature and humidity under both day and night  
66 conditions. A different intercomparison study was carried out at a site in Oklahoma, USA, by  
67 Jensen et al. (2016). They showed that the RS92 and RS41 measurements agreed much  
68 better than the manufacturer-specified combined uncertainties. Their results also indicated  
69 that the RS41 measurements of temperature and humidity appeared to be less sensitive to  
70 solar heating than those made with the RS92.

71 The accuracy of the pressure measured with the model RS41-SGP, however, has not  
72 yet been examined, nor has a comparison been made between the RS41 and RS92  
73 radiosondes in the marine atmosphere. Unlike the atmosphere over land, the marine  
74 atmosphere is less affected by topography and the greater temperature variations of the  
75 land surface. As a result, phenomena such as convection and precipitation and their diurnal  
76 cycles over the oceans are different from those over land (e.g. Yang and Slingo, 2001;  
77 Minobe and Takebayashi, 2015). We performed a total of 36 intercomparison flights during  
78 two cruises of R/V *Mirai* of the Japan Agency for Marine-Earth Science and Technology  
79 (JAMSTEC) in 2015. Our observations covered a wide range of latitudes over the oceans,  
80 an important consideration from the standpoint of confirming the performance of the RS41.

81 We describe the cruises and the methodology of the intercomparison observations in Sect.  
82 2. Section 3 shows the results of the comparisons. In Sect. 4, we focus on the data obtained  
83 in the tropics and further discuss the reasons for the differences between the RS41 and  
84 RS92 results. Section 5 is a summary of the study.

## 85 **2 Intercomparison experiment**

### 86 **2.1 Cruises**

87 The intercomparison observations were performed by launching both the RS41 and RS92  
88 radiosondes tied to one balloon (referred to as a “twin-radiosonde” flight) during the  
89 MR15-03 and MR15-04 cruises of R/V *Mirai*. In the case of the MR15-03 cruise, the vessel  
90 departed from Hachinohe, Japan, on 26 August, cruised the Arctic Ocean from 6  
91 September to 3 October (Nishino et al., 2015), and returned to Hachinohe on 21 October.

92 The twin-radiosonde flights were launched 9 times in the Chukchi Sea, 4 times in the Bering  
93 Sea, and 5 times in the northwestern Pacific (Fig. 1a and Table 2). The MR15-04 cruise  
94 was for tropical meteorological research, and the vessel stayed near 4°04' S, 101°54' E off  
95 Bengkulu, west of Sumatra Island, in the Indian Ocean during 23 November to 17  
96 December for stationary observations, including 16 twin-radiosonde flights (Katsumata et  
97 al., 2015). We also conducted intercomparison observations twice in the western Pacific on  
98 the way from Japan to the site off Sumatra (Fig. 1b and Table 2). ~~(Note that the cruise~~  
99 ~~reports [Katsumata et al., 2015; Nishino et al., 2015] were written based on RS92 data~~

100 ~~wrongly processed with an older version of DigiCORA. The preliminary analyses in the~~  
101 ~~cruise reports should be disregarded.)~~

## 102 **2.2 Methods**

103 We used radiosonde models RS92-SGPD and RS41-SGP in this study. Their nominal  
104 accuracies are summarized in Table 1. Whereas the RS41-SG radiosonde used in the  
105 previous studies (Motl, 2014; Jauhiainen et al., 2014; Jensen et al., 2016) derived pressure  
106 from Global Positioning System (GPS) data with no pressure sensor, the RS41-SGP has a  
107 pressure sensor consisting of a silicon capacitor. The pressure and height data analyzed in  
108 this study were measured directly and derived from the hypsometric equation, respectively.  
109 Note that GPS-derived pressure and height were not used, unlike in the previous studies.  
110 Two different DigiCORA systems were used on R/V *Mirai* for the simultaneous RS92 and  
111 RS41 soundings. The receiving system (MW41) used for the RS41 included a processor  
112 (SPS331), processing and recording software (MW41 v2.2.1), GPS antenna (GA20), and  
113 UHF antenna (RB21), which was part of the ASAP sounding station permanently installed  
114 on R/V *Mirai*. The RS41 sensors were calibrated with a new calibrator (RI41) and a  
115 barometer (PTB330). In contrast, we used a previous generation system for the RS92: the  
116 receiving system (MW31) included a processor (SPS311), software (DigiCORA v3.64),  
117 GPS antenna (GA31), and UHF antenna (RM32). The instrumentation was temporarily  
118 placed in or on the aft wheelhouse. The RS92 sensors were calibrated with a calibrator

119 (GC25) and a PTB330 barometer. Because version 3.61 of DigiCORA was incorrectly used  
120 during the cruises, all RS92 sounding data were simulated with DigiCORA v3.64 after the  
121 cruises.

122 The RS41 and RS92 radiosondes were directly attached to each other with sticky  
123 tape (Fig. 2) instead of hanging them from the two ends of a rod (Jensen et al., 2016) to  
124 facilitate the launching operations on the rocking ship deck. The two radiosondes were  
125 hung from a single 350g Totex balloon with the cord of the RS41 radiosonde. The ascent  
126 rates were approximately  $5 \text{ m s}^{-1}$  and  $4 \text{ m s}^{-1}$  during the MR15-03 and MR15-04 cruises,  
127 respectively (Table 2). Whereas nighttime twin-radiosonde flights could be carried out only  
128 once during the MR15-03 cruise owing to operations associated with oceanographic  
129 observations, we performed eight nighttime flights during the MR15-04 cruise (Fig. 1c and  
130 Table 2). In addition information about surface meteorological state, Table 2 lists convective  
131 available potential energy (CAPE), convective inhibition (CIN), and precipitable water (PW)  
132 calculated from RS41 data. CAPE and CIN were calculated for an air parcel corresponding  
133 to an average over the lowest 50 hPa.

134 A number of issues were addressed in post-processing the sounding data. During  
135 flight No. 33 (02:50 UTC on 16 Dec.), the radiosondes ~~moved up and down around a~~  
136 ~~temperature of  $0^{\circ}\text{C}$ , perhaps because the balloon froze~~ oscillated vertically about the  $0^{\circ}\text{C}$   
137 level likely due to icing on the balloon, and hence only the data before the up-and-down  
138 motion were analyzed in this study. In the case of flight No. 9 (05:30 UTC on 16 Sep.), we



139 delayed the measurement time of the RS41 by 17 s in the analysis because the twin  
140 radiosondes flew horizontally just after launching, and the automatic determinations of the  
141 starting times disagreed between the RS92 and RS41. Because the pressure values  
142 measured with the PTB330 barometer for the calibration of the RS92 had a bias of 0.18  
143 hPa before the launch of the No. 5 radiosondes, we subtracted 0.18 hPa from the observed  
144 pressure values of the RS92 No. 1–4 radiosondes when the data were analyzed. The  
145 balloon release detection mode was changed from automatic to manual during the  
146 MR15-04 cruise, and the starting times of the RS92 and RS41 radiosondes during the  
147 MR15-04 cruise generally appeared to differ slightly. Therefore, the measurement times of  
148 all the RS92 radiosonde data during the MR15-04 cruise were delayed by 1.7 s in the  
149 analysis.

### 150 **3 Results**

151 ~~For easier~~To facilitate comparison with the results of Jensen et al. (2016), we interpolated  
152 the RS92 radiosonde profiles to the same time step as the RS41 profiles, and calculated  
153 differences between them at each 10-m vertical grid based on the RS41 radiosonde heights  
154 (Fig. 3). The vertical axis of Fig. 3 is therefore nearly equivalent to the passage of time. The  
155 biases, standard deviations, and root mean square (RMS) differences were all smaller than  
156 the combined uncertainties, except that the RMS differences of pressure above 100 hPa  
157 exceeded 0.6 hPa (Table 3). For temperature and wind speeds, the biases and RMS

158 differences in our experiments were nearly the same as those of Jensen et al. (2016), but  
159 the differences of pressure and relative humidity were much larger in our study.

### 160 3.1 Pressure

161 The pressure difference between the RS41 and RS92 radiosondes increased as the  
162 radiosondes rose to an altitude of about 5 km but averaged an almost constant 0.5–0.6 hPa  
163 above that altitude (Fig. 3a). The 90th-percentile line revealed that the sensor-measured  
164 RS41 pressure was lower than the RS92 for more than 90 % of the measurements above 5  
165 km. The percentage of the pressure differences that exceeded the combined uncertainty  
166 (Table 1) was 13.7 % below 100 hPa but 50.9 % above 100 hPa. The bias of pressure  
167 causes the bias of geopotential height (Fig.3b). The height difference increased with the  
168 altitude: The median of the RS41 height was greater than that of the RS92 by  
169 approximately 35 m at an altitude of 15 km, and 100 m at 22 km.

170 We also checked the GPS-derived pressure of the RS41 radiosondes. Figure 4  
171 shows the difference between the RS92 pressure and the RS41 GPS-derived one. The use  
172 of the GPS-derived pressure reduced the bias by approximately 0.2 hPa above an altitude  
173 of 15 km, but there was still a bias of 0.4 hPa or more at most of altitudes. The median of  
174 the difference in Fig.4 was almost the same as in Fig.3a around an altitude of 5 km. The  
175 use of the GPS did not essentially improve the pressure bias. This is different from the  
176 results of Jensen et al. (2016).

## 177 3.2 Relative humidity

178 The median of the relative humidity differences peaked at approximately 2 %RH near  
179 10 km (Fig. [3b3c](#)), a result consistent with the data of Jensen et al. (2016). The humidity  
180 difference was also large near the sea surface in our analysis. For 13.0 % of the  
181 measurements, the absolute value of the difference exceeded 4.0 %RH, which is the  
182 combined uncertainty of the RS41-SGP. One noteworthy feature of Fig. [3b-3c](#) is that there  
183 were quite large differences of relative humidity at a height of about 17 km, although the  
184 median difference was less than 0.5 %RH. Figure [4-5](#) shows the relationship between the  
185 humidity difference and temperature for each category of relative humidity. During both the  
186 MR15-03 and MR15-04 cruises, the RS41 radiosonde ~~tended to record~~ed a higher mean  
187 relative humidity ~~than relative to~~ the RS92 for all humidity ranges. The humidity difference  
188 peaked at around  $-40^{\circ}\text{C}$ , a pattern similar to Fig. 17 of Jensen et al. (2016). The  
189 differences were relatively small in the range of  $-50^{\circ}$  to  $-70^{\circ}\text{C}$ , but the RS41 humidity was  
190 much higher than the RS92 at temperatures below  $-80^{\circ}\text{C}$  (Fig. [4b5b](#)). The atmosphere  
191 associated with temperatures below  $-80^{\circ}\text{C}$  corresponds to the tropopause in the tropics,  
192 where the greatest differences were apparent at altitudes of about 17 km (Fig. [3b3c](#)).

## 193 3.3 Temperature

194 In the case of temperature, although there was a slight positive bias below an altitude of 10  
195 km, the median of the differences was within  $\pm 0.12^{\circ}\text{C}$  below an altitude of 26 km (Fig. [3c3d](#)).

196 The median exceeded 0.5°C above 27 km, but only four flights reached that height, and the  
197 large median was attributable to differences on two of the flights (No. 23 and 24). The  
198 percentages of the temperature difference that exceeded the combined uncertainty were  
199 4.0 % below 16 km and 5.9 % above 16 km. Figure ~~3e-3d~~ also shows that the standard  
200 deviation of the temperature differences was smaller at altitudes below 16 km, but there  
201 were quite large standard deviations near the surface and at altitudes of about 1.3 km and  
202 5.3 km because of some outliers. The extreme temperature difference, which reached  
203 2.75°C at an altitude of 1.27 km, was observed on 10 December in the tropics (Fig. ~~5a6a~~).  
204 The RS92 temperature became much lower than the RS41 just after the radiosondes  
205 passed through a saturated layer into a dry layer. The greater reduction of the RS92  
206 temperature was probably due to the “wet-bulbing” effect mentioned by Jensen et al. (2016),  
207 who indicated that the sequential pulse heating method with relatively long non-heating  
208 periods may not be sufficient to eliminate icing/wetting of the RS92 sensor. A large  
209 temperature difference that was likely caused by the wet-bulbing effect was also observed  
210 in a sounding in the Arctic, although the maximum difference was less than 0.75°C (Fig.  
211 ~~5b6b~~).

212 Figure ~~6-7~~ shows the cases of extreme temperature differences that contributed to the  
213 greater standard deviation and cannot be explained by the wet-bulbing effect. For the flight  
214 on 11 December (Fig. ~~6a7a~~), there was a large temperature discrepancy inside the  
215 saturated layer. In that case, the radiosondes were launched in heavy rain, and the ascent

216 rate dropped to nearly zero at approximately 5.4 km, probably because of rain or snow and  
217 freezing of the balloon. Furthermore, the horizontal wind speed was less than  $3.0 \text{ m s}^{-1}$   
218 around this altitude. As a result, the temperature sensors were presumably not ventilated  
219 sufficiently. In the case of the flights on 1 and 3 December (Fig. ~~6b~~7b and ~~6e~~7c), the RS41  
220 temperatures were higher than the RS92 by more than  $1.0^{\circ}\text{C}$  near the surface. Because  
221 the surface reference air temperatures were close to the RS92 temperatures at the lowest  
222 level, we suspect that the RS41 temperatures were too high. These large temperature  
223 differences lead to enormous discrepancies in CAPE:  $864.6 \text{ J kg}^{-1}$  for No.22, and  $1819.0 \text{ J}$   
224  $\text{kg}^{-1}$  for No.23. Yoneyama et al. (2002) have indicated that ship body heating can affect  
225 radiosonde sensors. However, that effect was restricted to within several tens of meters of  
226 the sea surface in their experiments. Although we cannot completely exclude the possibility  
227 that the temperature sensors of the two RS41 radiosondes were improperly heated by the  
228 body of the ship or direct insolation or improper handling near the surface, the reason for  
229 these large discrepancies remains unclear.

### 230 **3.4 Wind speed**

231 Vertical profiles of the wind speed differences are shown in Fig. ~~3d~~3e and ~~3e~~3f. The  
232 percentages of the differences in the zonal and meridional wind speeds that exceeded  $0.5$   
233  $\text{m s}^{-1}$  were 1.9 % and 1.5 %, respectively. Although both the zonal and meridional wind  
234 speeds agreed to within  $0.5 \text{ m s}^{-1}$  for almost all measurements, several spikes can be seen

235 in the standard deviations and percentiles. In half of all flights, the magnitude of the  
236 difference of the horizontal wind speed exceeded  $1.0 \text{ m s}^{-1}$  for a brief moment. The wind  
237 speed data in our soundings were noisier than those reported by Jensen et al. (2016).

238

## 239 **4 Discussion**

### 240 **4.1 Day-night differences**

241 Figure [7-8](#) compares the differences between daytime (10 flights) and nighttime (8 flights)  
242 for the soundings during the MR15-04 cruise. The median of the pressure difference was  
243 greater in the day than at night above an altitude of 4.5 km (Fig. [7a8a](#)). The median of the  
244 nighttime differences was close to that of the daytime flights in the Arctic cruise below an  
245 altitude of 15 km, the implication being that the day-night difference might reflect some  
246 effect of solar heating.

247 The median profiles of temperature differences in the day and night were close to  
248 each other, with slightly larger differences in the night at altitudes of 5–15 km (Fig. [7b8b](#)).  
249 The daytime difference became greater above approximately 24 km, a pattern similar to the  
250 results of Jensen et al. (2016). According to them, the difference in the radiation correction  
251 schemes between the RS92 and RS41 may be the dominant cause of these temperature  
252 differences, particularly at high solar elevation angles and low pressures.

253 The median of the relative humidity difference was larger during the day than at night

254 from the surface to an altitude of 20 km and was especially large at an altitude of about 17  
255 km (Fig. ~~7e~~8c). The very large difference (RS41 > RS92) in relative humidity around the  
256 tropopause shown in Figs. 3c and ~~4b~~5b occurred in the daytime. This pattern is consistent  
257 with the results of Jauhiainen et al. (2014), who indicated that the difference was largely  
258 due to the dissimilar approaches used to compensate for the heating effect of solar  
259 radiation on the humidity sensor. Similar dry biases were reported for the RS92 radiosonde  
260 with the earlier version of DigiCORA (Vömel et al., 2007; Yoneyama et al., 2008), although  
261 the dry bias was generally absent from later observations (Ciesielski et al., 2014; Yu et al.,  
262 2015) because the bias due to solar heating was removed by a correction scheme included  
263 in the v3.64 software or developed by Wang et al. (2013). Figure ~~8~~9 shows the relative  
264 difference of relative humidity in the daytime between the RS92 and RS41 radiosondes.  
265 The relative difference is defined to be the relative humidity difference expressed as a  
266 percentage of the RS41 relative humidity. The relative difference was small in the lower  
267 troposphere and became greater as the radiosondes rose higher. Its median peaked at  
268 -36.9 % at an approximate altitude of 19 km. This pattern of the vertical profile of relative  
269 difference is similar to that between the RS92 radiosonde and a reference instrument  
270 shown by Vömel et al. (2007), but the values in Fig. ~~8~~9 are less than half of those in Fig. 6  
271 of Vömel et al. (2007) because the RS92 DigiCORA v3.64 and RS41 relative humidity data  
272 are already inherently better.

273 We evaluated how the differences between the two types of radiosonde affected

CAPE, CIN, and PW (Table 4). CAPE tended to be larger when the RS92 was used in the nighttime. This was due to slightly higher temperature of RS92 near the surface (Fig.8b). On the other hand, in the daytime the RS41 CAPE was larger than the RS92 and the RS41 CIN was smaller than the RS92. The day-night differences in the CAPE and CIN biases were caused by the difference in the humidity bias between daytime and nighttime. The near-surface humidity of the RS41 was larger than that of the RS92 in the daytime (Fig.8c). The larger pressure bias in daytime (Fig.8a), which means to thicken an atmospheric layer in the RS41 observation, also may contribute to the daytime bias of CAPE. Although the bias of PW was less than 1.0 mm, the daytime humidity difference between the RS41 and RS92 affected PW. The ratio of the RS41 to the RS92 PW was dependent on solar altitude angle (Fig.10), similar to the general shape of the dependence indicated by Miloshevich et al. (2009) (their Fig.4a), suggesting that the humidity bias was mainly related with solar heating.

## 4.2 Humidity correction

Figures ~~7c~~8c, 9 and ~~8~~10 imply that a small dry bias still remains in the RS92 radiosonde observations. We attempted to correct the RS92 relative humidity obtained during the MR15-04 cruise by using the RS41 as a reference instrument. However, this is not based on an assertion that the RS42 measurements must be true values. There is no independent evidence to judge which radiosonde was more accurate. The RS41 relative humidity was



larger than the RS92 at an altitude between 3-13 km (Fig.8c), suggesting that the RS41 humidity also have a slight moist bias that is unrelated to the radiation correction scheme. The correction attempted in this subsection is a proposal to bridge the gap in relative humidity between the RS41 and RS92 radiosondes.

We used the cumulative distribution function (CDF) matching method proposed by Nuret et al. (2008) and Ciesielski et al. (2009) to make the correction. The details of this method can be found in Ciesielski et al. (2009). We first created CDFs of relative humidity for the RS92 and RS41 using temperature bins of 20°C between +30° and -90°C (10 to 30°C, -10 to 10°C, -30 to -10°C, -50 to -30°C, -70 to -50°C, and -90 to -70°C) using 5hPa radiosonde data in 5%RH intervals. Figure 9-11 shows the CDFs of the RS92 and RS41 in the temperature range -90 to -70°C as an example. The frequency of lower relative humidity was greater for the RS92 in this temperature range, which includes the tropopause (Fig. 9a-11a). We then, for example, paired the RS92 value of 27.50 %RH at the 71.23th percentile with the corresponding RS41 value at this same percentile. The RS41 relative humidity at the 71.23th percentile was 36.43 %RH, and the difference between 36.43 %RH and 27.50 %RH (= +8.93 %RH) was the bias correction for the RS92 value of 27.5 %RH. Figure 9b-11b shows the bias correction over the entire relative humidity range for temperatures of -90 to -70°C.

Table 4-5 shows the daytime bias correction for the entire ranges of temperatures and relative humidityes. The correction was seldom more than 5 %RH when the RS92

313 temperature exceeded  $-60^{\circ}\text{C}$ . The correction was large for RS92 radiosonde values in the  
314 range 15–50 %RH and temperatures of  $-80^{\circ}\text{C}$ , with a maximum of +8.93 %RH. This  
315 pattern is similar to that of the correction table for the RS80 radiosonde in the daytime  
316 reported by Ciesielski et al. (2010) (their Fig. 7b), but the values in Table 4–5 are much  
317 smaller. We corrected the daytime RS92 relative humidity values obtained during the  
318 MR15-04 cruise using Table 45. The correction value for an arbitrary RS92 measurement  
319 can be obtained by linear two-dimensional interpolation using Table 4–5 and the RS92  
320 temperature and relative humidity. Figure 40–12 shows median profiles of the differences  
321 between the RS92 and RS41 radiosondes before and after the correction. Although the  
322 median of the magnitude of the differences still exceeded 2.0 %RH around 120, 150, and  
323 560 hPa, most of the medians were within  $\pm 1.0$  %RH. The mean of the relative humidity  
324 difference of the 5hPa interval data was  $-2.02$  %RH if no correction was made; this  
325 difference was reduced to  $-0.01$  %RH after the correction.

## 326 5 Conclusions

327 To examine differences between the RS41 and RS92 radiosondes, a total of 36  
328 twin-radiosonde flights were performed over the Arctic Ocean, Bering Sea, northwestern  
329 Pacific Ocean, and the tropical Indian Ocean during two cruises of R/V *Mirai* in 2015. We  
330 used the model RS41-SGP radiosonde, which has a pressure sensor, unlike previous  
331 studies that used the RS41-SG, which has no pressure sensor.

332       The biases, standard deviations, and RMS of the differences between the RS41 and  
333 RS92 over all flights and heights were smaller than the nominal combined uncertainties of  
334 the RS41, except that the RMS differences of pressure above 100 hPa exceeded 0.6 hPa.  
335 Whereas the biases and the RMS differences of temperature and wind speeds were close  
336 to those reported by Jensen et al. (2016), the differences of pressure and relative humidity  
337 were greater in our experiments. The pressure difference increased as the radiosondes  
338 rose higher; the median and mean were 0.5–0.6 hPa at altitudes above 5 km. This pressure  
339 difference corresponded to a geopotential height difference of more than 35 m above an  
340 altitude of 15 km. A comparison between daytime and nighttime flights in the tropics  
341 revealed that the pressure difference was systematically larger in the day than at night at  
342 altitudes above 4.5 km, the suggestion being that there was some effect of solar heating on  
343 the pressure measurements. The exact reason, however, is unclear.

344       The RS41 and RS92 temperature measurements in general agreed better than the  
345 combined uncertainties, but there were some noteworthy exceptions. One possible reason  
346 for the noteworthy discrepancies is the wet-bulbing effect described by Jensen et al. (2016).  
347 In a dry layer just above a saturated layer, the RS92 temperature sensor was cooled too  
348 much by evaporation. The RS41 temperature appeared to be less sensitive to this  
349 wet-bulbing effect. This phenomenon was confirmed in both the tropics and Arctic. During  
350 heavy rain and weak wind conditions, the stagnation of the balloon probably suppressed  
351 the ventilation around the temperature sensors, the result being an extreme temperature

352 difference.

353       The median of the relative humidity differences at all altitudes was only a little more  
354 than 2 %RH. However, there were quite large differences at an altitude of about 17 km.  
355 These large differences occurred in the daytime around the tropical tropopause, where the  
356 temperature was below  $-80^{\circ}\text{C}$ . The reason for this dry bias may be that there was some  
357 remnant of the error of the RS92 radiosonde solar radiation correction. The differences in  
358 humidity affected the calculation of CAPE, CIN, and PW, and we confirmed the day-night  
359 difference of these variables. We attempted to correct the RS92 relative humidity data  
360 obtained in the daytime during the MR15-04 cruise by using the CDF matching method,  
361 and the corrected RS92 relative humidity agreed well with the RS41 values.

362       Our results showed that measurements with the RS41 radiosonde satisfied the  
363 performance specifications of the manufacturer in most cases over both the tropical and  
364 polar oceans. The RS41 temperature and humidity sensors appeared to be unaffected by  
365 the solar radiation correction error and the wet-bulbing effect. Some concerns, however,  
366 remain. Specifically, the reasons for the pressure bias in the upper layer and the two cases  
367 of extreme temperature discrepancies that occurred below an altitude of several hundred  
368 meters are unknown. Further experiments will be necessary to address these issues, and  
369 users should be cognizant of these concerns.

## 370 **6 Data availability**

371 The sounding dataset and the ship-observed surface meteorology are expected to be  
372 released just two years after the cruises (October 2017 for the MR15-03, and December  
373 2017 for the MR15-04) from the website of the Data Research System for Whole Cruise  
374 Information (DARWIN) in JAMSTEC (<http://www.godac.jamstec.go.jp/darwin/e>) in accord  
375 with the cruise data policy of JAMSTEC.

376

#### 377 Author contributions

378 All co-authors contributed to designing the experiments and preparing for the observation  
379 cruises. Y. Kawai, M. Katsumata, and K. Oshima participated in the R/V *Mirai* cruises and  
380 carried out the radiosonde soundings. K. Oshima reprocessed the RS92 data. M.  
381 Katsumata calculated CAPE, CIN, and PW. Y. Kawai mainly analyzed the data and  
382 prepared the manuscript with contributions from all co-authors.

383

384 *Acknowledgments.* The authors sincerely thank the captains, crews, and observation  
385 technicians of the R/V *Mirai* and all colleagues who helped with the experiments. The  
386 authors are also grateful to K. Yoneyama of JAMSTEC for valuable advice, especially for  
387 advice concerning the humidity correction. This study was supported by the Japan Society  
388 for the Promotion of Science (JSPS) Grants-in-Aid for Scientific Research (A), (B), and (C)  
389 (KAKENHI) Grant Number 24241009, 16H04046, and 16K05563.

390

391 **References**

- 392 Bodeker, G. E., Bojinski, S., Cimini, C., Dirksen, R. J., Haeffelin, M., Hannigan, J. W., Hurst,  
393 D. F., Leblanc, T., Madonna, F., Maturilli, M., Mikalsen, A. C., Philpona, R., Reale, T.,  
394 Siedel, D. J., Tan, D. G. H., Thorne, P. W., Vömel, H., and Wang, J.: Reference upper-air  
395 observations for climate: From concept to reality, B. Am. Meteorol. Soc., 97, 123-135,  
396 doi:10.1175/BAMS-D-14-00072.1, 2016.
- 397 Ciesielski, P. E., Johnson, R. H., and Wang, J: Correction of humidity biases in Vaisala  
398 RS80-H sondes during NAME, J. Atmos. Ocean. Tech., 26, 1763-1780,  
399 doi:10.1175/2009JTECHA1222.1, 2009.
- 400 Ciesielski, P. E., Chang, W.-M., Huang, S. -C., Johnson, R. H., Jou, B. J. -D., Lee, W. -C.,  
401 Lin, P. -H., Liu, C. -H., and Wang, J.: Quality-controlled upper-air sounding dataset for  
402 TiMREX/SoWMEX: Development and corrections, J. Atmos. Ocean. Tech., 27,  
403 1802-1821, doi:10.1175/2010JTECHA1481.1, 2010.
- 404 Ciesielski, P. E., Yu, H., Johnson, R. H., Yoneyama, K., Katsumata, M., Long, C. N., Wang,  
405 J., Loehrer, S. M., Young, K., Williams, S. F., Brown, W., Braun, J., and Van Hove, T.:  
406 Quality-controlled upper-air sounding dataset for DYNAMO/CINDY/AMIE: Development  
407 and corrections, J. Atmos. Ocean. Tech., 31, 741-764, doi:10.1175/JTECH-D-13-00165.1,  
408 2014.
- 409 Fujita, M., Kimura, F., Yoneyama, K., and Yoshizaki, M.: Verification of precipitable water  
410 vapor estimated from shipborne GPS measurements, Geophys. Res. Lett., 35, L13803,

doi:10.1029/2008GL033764, 2008

Inoue, J., Enomoto, T., and Hori, M. E.: The impact of radiosonde data over the ice-free Arctic Ocean on the atmospheric circulation in the Northern Hemisphere, *Geophys. Res. Lett.*, 40, 864-869, doi:10.1002/grl.50207, 2013.

Inoue, J., Yamazaki, A., Ono, J., Dethloff, K., Maturilli, M., Neuber, R., Edwards, P., and Yamaguchi, H.: Additional Arctic observations improve weather and sea-ice forecasts for the Northern Sea Route, *Sci. Rep.*, 5, 16868, doi:10.1038/srep16868, 2015.

Jauhiainen, H., Survo, P., Lehtinen, R., and Lentonen, J.: Radiosonde RS41 and RS92 key differences and comparison test results in different locations and climates. *TECO-2014, WMO Technical Conference on Meteorological and Environmental Instruments and Methods of Observations*, Saint Petersburg, Russian Federation, 7–9 July 2014, P3(16), 2014.

Jensen, P. M., Holdridge, D. J., Survo, P., Lehtinen, R., Baxter, S., Toto, T., and Johnson, K. L.: Comparison of Vaisala radiosondes RS41 and RS92 at the ARM Southern Great Plains site, *Atmos. Meas. Tech.*, 9, 3115-3129, doi:10.5194/amt-9-3115-2016, 2016.

Katsumata, M., and coauthors: *R/V Mirai Cruise Report MR15-04*, Cruise Rep., Japan Agency for Marine-Earth Science and Technology, Yokosuka, Japan, 241.pp, 2015.

(Available from [http://www.godac.jamstec.go.jp/catalog/data/doc\\_catalog/media/MR15-04\\_all.pdf](http://www.godac.jamstec.go.jp/catalog/data/doc_catalog/media/MR15-04_all.pdf))

Kawai, Y., Tomita, H., Cronin, M. F., and Bond, N. A.: Atmospheric pressure response to

431 mesoscale sea surface temperature variations in the Kuroshio Extension: In situ  
 432 evidence, *J. Geophys. Res. Atmos.*, 119, 8015-8031. doi:10.1002/2013JD021126, 2014.

433 Maturilli, M., and Kayser, M.: Arctic warming, moisture increase and circulation changes  
 434 observed in the Ny-Ålesund homogenized radiosonde record, *Theor. Appl. Climatol.*,  
 435 doi:10.1007/s00704-016-1864-0, 2016.

436 Miloshevich, L. M., Vömel, H., Whiteman, D. N., and Leblanc, T.: Accuracy of assessment  
 437 and correction of Vaisala RS92 radiosonde water vapor measurement, *J. Geophys. Res.*,  
 438 114, D11305, doi:10.1029/2008JD011565, 2009.

439 Minobe, S., and Takebayashi, S.: Diurnal precipitation and high cloud frequency variability  
 440 over the Gulf Stream and over the Kuroshio, *Clim. Dyn.*, 44, 2079-2095,  
 441 doi:10.1007/s00382-014-2245-y, 2015.

442 Motl, M.: Vaisala RS41 trial in the Czech Republic, *Vaisala News*, 192, 14-17, 2014.

443 Nishino, S., and coauthors: R/V Mirai Cruise Report MR15-03, Cruise Rep., Japan Agency  
 444 for Marine-Earth Science and Technology, Yokosuka, Japan, 297.pp, 2015. (Available  
 445 from  
 446 [http://www.godac.jamstec.go.jp/catalog/data/doc\\_catalog/media/MR15-03\\_leg1\\_all.pdf](http://www.godac.jamstec.go.jp/catalog/data/doc_catalog/media/MR15-03_leg1_all.pdf))

447 Nuret, M., Lafore, J.-P., Bock, O., Guichard, F., Agusti-Panareda, A., N'Gamini, J.-B., and  
 448 Redelsperger, J.-L.: Correction of humidity bias for Vaisala RS80-A sondes during the  
 449 AMMA 2006 observing period, *J. Atmos. Ocean. Tech.*, 25, 2152-2158,  
 450 doi:10.1175/2008JTECHA1103.1, 2008.



451 Thorne, P. W., Parker, D. E., Tett, S. F. B., Jones, P. D., McCarthy, M., Coleman, H., and  
 452 Brohan, P.: Revisiting radiosonde upper air temperatures from 1958 to 2002, *J. Geophys.*  
 453 *Res.*, 110, D18105, doi:10.1029/2004JD005753, 2005.

454 Vömel, H., Selkirk, H., Miloshevich, L., Valverde-Canossa, J., Valdés, J., Kyrö, E., Kivi, R.,  
 455 Stolz, W., Peng, G., and Diaz, J. A.: Radiation dry bias of the Vaisala RS92 humidity  
 456 sensor, *J. Atmos. Ocean. Tech.*, 24, 953-963, doi:10.1175/JTECH2019.1, 2007.

457 Wang, J., Zhang, L., Dai, A., Immler, F., Sommer, M., and Vömel, H.: Radiation dry bias  
 458 correction of Vaisala RS92 humidity data and its impacts on historical radiosonde data, *J.*  
 459 *Atmos. Ocean. Tech.*, 30, 197-214, doi:10.1175/ JTECH-D-12-00113.1, 2013.

460 Yang, G.-Y., and Slingo, J.: The diurnal cycle in the tropics, *Mon. Wea. Rev.*, 129, 784-801,  
 461 doi:10.1175/1520-0493(2001)129<0784:TDCITT>2.0.CO;2, 2001.

462 Yoneyama, K., Hanyu, M., Sueyoshi, S., Yoshiura, F., and Katsumata, M.: Radiosonde  
 463 observation from the ship in the tropical region, *Report of Japan Marine Science and*  
 464 *Technology Center*, 45, 31-39, 2002. (Available from  
 465 [http://www.jamstec.go.jp/res/ress/yoneyamak/PDFs/Yoneyama-etal\\_2002\\_JAMSTECR.](http://www.jamstec.go.jp/res/ress/yoneyamak/PDFs/Yoneyama-etal_2002_JAMSTECR.pdf)  
 466 pdf)

467 Yoneyama, K., Fujita, M., Sato, N., Fujiwara, M., Inai, Y., and Hasebe, F.: Correction for  
 468 radiation dry bias found in RS92 radiosonde data during the MISMO field experiment,  
 469 *SOLA*, 4, 13-16, doi:10.2151/sola.2008-004, 2008.

470 Yu, H., Ciesielski, P. E., Wang, J., Kuo, H.-C., Vömel, H., and Dirksen, R.: Evaluation of

471 humidity correction methods for Vaisala RS92 tropical sounding data, J. Atmos. Ocean.  
472 Tech., 32, 397–411, doi:10.1175/JTECH-D-14-00166.1, 2015.

473

474

475 **Table 1.** Nominal accuracies of the radiosondes according to the manufacturer.

476

		RS41-SGP	RS92-SGPD
Weight		113 g	280 g
Combined uncertainty in sounding (2-sigma confidence level (95.5 %) cumulative uncertainty)	Temperature	0.3°C < 16 km 0.4°C > 16 km	0.5°C
	Relative humidity	4 %RH	5 %RH
	Pressure		1.0 > 100 hPa 0.6 < 100 hPa
	Temperature <sup>a</sup>	0.15°C > 100 hPa 0.30°C < 100 hPa	0.2°C > 100 hPa 0.3°C 100–20 hPa 0.5°C < 20 hPa
	Relative humidity <sup>a</sup>		2 %RH
Reproducibility in sounding (standard deviation of differences in twin soundings)	Pressure		0.5 > 100 hPa 0.3 < 100 hPa
	Wind speed		0.15 m/s
	Wind direction <sup>b</sup>		2°

477 <sup>a</sup> Ascent rate above 3 m s<sup>-1</sup>

478 <sup>b</sup> Wind speed above 3 m s<sup>-1</sup>

**Table 2.** Date, position (latitude and longitude), ~~and~~ surface meteorological state (pressure, temperature, relative humidity, wind direction, and wind speed), CAPE, CIN, and PW when each twin-radiosonde was launched. Line under UTC time denotes nighttime.

<u>Cruise</u>	No.	Date	Time (UTC)	<u>Time</u> <u>(LT)</u>	Lat. (°N)	Lon. (°E)	Pressure (hPa)	Temp. (°C)	RH (%)	Wind dire. (°)	Wind speed (m s <sup>-1</sup> )	<u>RS41</u> Maximum height (m)	Mean ascent rate (m s <sup>-1</sup> )	<u>RS41</u> <u>CAPE</u> (J kg <sup>-1</sup> )	<u>RS41 CIN</u> (J kg <sup>-1</sup> )	<u>RS41 PW</u> (mm)
<u>15-03</u>	1	27 Aug.	23:30	<u>9:30</u>	40.17 <del>0</del>	149.94 <del>4</del>	1011.7	15.9	69	23	7.1	26,734	4.06	<u>0</u>	<u>NA</u>	<u>14.3</u>
	2	28 Aug.	23:30	<u>9:30</u>	42.42 <del>3</del>	153.41 <del>3</del>	1010.7	14.0	70	306	11.2	23,328	4.42	<u>0.6</u>	<u>1.5</u>	<u>11.3</u>
	3	29 Aug.	23:30	<u>9:30</u>	44.83 <del>4</del>	157.19 <del>3</del>	1004.2	12.1	93	289	11.6	21,607	4.45	<u>0</u>	<u>NA</u>	<u>31.2</u>
	4	31 Aug.	23:32	<u>10:32</u>	49.93 <del>4</del>	165.75 <del>3</del>	999.6	10.9	93	275	5.6	19,380	4.74	<u>3.8</u>	<u>4.5</u>	<u>24.0</u>
	5	2 Sep.	23:30	<u>11:30</u>	55.49 <del>3</del>	175.34 <del>2</del>	1000.4	10.3	97	155	7.8	13,617	4.68	<u>3.7</u>	<u>0</u>	<u>22.9</u>
	6	4 Sep.	23:32	<u>11:32</u>	63.43 <del>29</del>	-172.92 <del>17</del>	1008.6	9.0	81	294	3.6	23,554	5.06	<u>0.2</u>	<u>0.7</u>	<u>19.9</u>
	7	<del>7-8</del> Sep.	5:30	<u>18:30</u>	71.05 <del>4</del>	-166.94 <del>37</del>	1015.9	1.3	83	342	6.7	22,872	5.22	<u>2.6</u>	<u>0.4</u>	<u>8.4</u>
	8	12 Sep.	23:30	<u>13:30</u>	72.48 <del>76</del>	-156.29 <del>89</del>	1009.8	-0.1	96	91	9.3	21,243	5.36	<u>0.1</u>	<u>0</u>	<u>12.8</u>
	9	16 Sep.	5:30	<u>19:30</u>	72.34 <del>4</del>	-156.18 <del>3</del>	1015.1	-1.7	86	46	5.4	22,298	5.33	<u>0</u>	<u>0.2</u>	<u>7.7</u>
	10	24 Sep.	23:31	<u>12:31</u>	73.21 <del>09</del>	-157.80 <del>4</del>	993.2	0.7	95	170	9.8	25,309	5.12	<u>0</u>	<u>0</u>	<u>13.1</u>
	11	28 Sep.	17:31	<u>6:31</u>	74.37 <del>69</del>	-166.57 <del>69</del>	987.8	-1.4	92	164	8.6	23,291	5.18	<u>9.4</u>	<u>0.3</u>	<u>6.8</u>
	12	28 Sep.	23:30	<u>12:30</u>	74.47 <del>66</del>	-168.18 <del>4</del>	982.0	-0.9	70	167	11.2	22,811	5.26	<u>0</u>	<u>NA</u>	<u>6.4</u>
	13	29 Sep.	5:30	<u>18:30</u>	74.00 <del>2</del>	-168.76 <del>55</del>	979.9	-2.3	80	210	9.9	19,338	5.25	<u>47.8</u>	<u>1.1</u>	<u>4.6</u>
	14	30 Sep.	<u>11:30</u>	<u>0:30</u>	70.38 <del>79</del>	-168.76 <del>55</del>	993.2	-2.1	89	282	7.0	19,897	5.16	<u>0</u>	<u>NA</u>	<u>5.1</u>
	15	30 Sep.	23:30	<u>12:30</u>	68.06 <del>4</del>	-168.83 <del>29</del>	1008.6	1.8	69	296	7.1	22,613	5.17	<u>25.2</u>	<u>1.0</u>	<u>5.3</u>
	16	4 Oct.	23:30	<u>12:30</u>	60.74 <del>2</del>	-167.78 <del>77</del>	1011.4	8.1	100	186	14.3	19,498	4.77	<u>0.3</u>	<u>0</u>	<u>20.6</u>
	17	11 Oct.	23:30	<u>11:30</u>	53.64 <del>39</del>	178.82 <del>4</del>	1006.8	6.3	90	10	3.8	25,051	5.17	<u>0.7</u>	<u>0.4</u>	<u>14.5</u>

	18	17 Oct.	23:30	<u>9:30</u>	41.790	154.884	1019.8	12.0	64	177	2.9	25,928	5.21	<u>0</u>	<u>NA</u>	<u>9.2</u>
<u>15-04</u>	19	10 Nov.	5:38	<u>14:38</u>	23.5765	136.764	1011.6	26.7	83	357	3.3	25,395	3.78	<u>1309.0</u>	<u>5.6</u>	<u>42.1</u>
	20	11 Nov.	5:39	<u>14:39</u>	19.210	134.814	1011.6	28.0	81	72	8.1	26,589	4.04	<u>1558.5</u>	<u>4.6</u>	<u>42.6</u>
	21	30 Nov.	8:29	<u>15:29</u>	-4.0876	101.8985	1006.2	28.5	75	202	4.2	22,184	3.95	<u>630.9</u>	<u>22.8</u>	<u>59.8</u>
	22	1 Dec.	5:30	<u>12:30</u>	-4.054	101.8987	1008.1	28.4	79	298	2.7	26,510	4.27	<u>2228.8</u>	<u>3.4</u>	<u>60.4</u>
	23	3 Dec.	5:29	<u>12:29</u>	-4.0767	101.893	1008.5	28.0	82	275	4.2	28,867	4.35	<u>3008.1</u>	<u>3.7</u>	<u>63.0</u>
	24	5 Dec.	2:30	<u>9:30</u>	-4.0769	101.883	1009.5	26.0	92	254	1.9	28,016	4.07	<u>645.1</u>	<u>15.9</u>	<u>64.6</u>
	25	5 Dec.	<u>17:45</u>	<u>0:45</u>	-4.0985	101.893	1008.6	27.4	86	80	1.3	26,822	3.98	<u>1531.4</u>	<u>1.0</u>	<u>64.7</u>
	26	6 Dec.	<u>20:26</u>	<u>3:26</u>	-4.0767	101.910	1005.8	27.9	85	139	6.2	27,518	3.97	<u>1393.3</u>	<u>23.0</u>	<u>63.9</u>
	27	8 Dec.	<u>14:29</u>	<u>21:29</u>	-4.0879	101.890	1010.5	27.9	82	126	3.0	26,965	4.26	<u>1357.2</u>	<u>0.8</u>	<u>63.4</u>
	28	9 Dec.	2:28	<u>9:28</u>	-4.053	101.8987	1010.0	27.4	81	298	1.9	27,123	4.32	<u>979.2</u>	<u>9.6</u>	<u>66.8</u>
	29	10 Dec.	<u>17:27</u>	<u>0:27</u>	-4.042	101.890	1009.1	27.0	87	6	1.4	24,650	4.40	<u>1324.6</u>	<u>0.3</u>	<u>63.3</u>
	30	11 Dec.	<u>14:20</u>	<u>21:20</u>	-4.053	101.873	1008.0	25.5	98	5	10.3	15,050	6.62	<u>162.5</u>	<u>86.9</u>	<u>78.4</u>
	31	13 Dec.	<u>20:28</u>	<u>3:28</u>	-4.0659	101.894	1006.1	28.1	77	324	6.2	20,798	3.57	<u>887.1</u>	<u>12.5</u>	<u>60.0</u>
	32	15 Dec.	5:28	<u>12:28</u>	-4.0545	101.90896	1007.9	27.6	82	339	8.6	23,698	4.25	<u>1229.5</u>	<u>1.5</u>	<u>61.5</u>
	33	16 Dec.	2:50	<u>9:50</u>	-4.0657	101.8986	1010.3	25.0	94	310	5.2	4,803	2.48	<u>0</u>	<u>0.1</u>	<u>54.3</u>
	34	16 Dec.	<u>14:22</u>	<u>21:22</u>	-4.062	101.8989	1010.1	26.2	90	11	7.9	21,629	4.48	<u>1030.4</u>	<u>0.4</u>	<u>57.6</u>
	35	17 Dec.	5:28	<u>12:28</u>	-4.053	101.90896	1008.2	28.2	72	278	1.4	21,607	3.61	<u>379.5</u>	<u>24.1</u>	<u>48.2</u>
	36	17 Dec.	<u>20:27</u>	<u>3:27</u>	-5.173	101.413	1007.2	28.2	79	303	6.0	24,944	3.70	<u>2035.6</u>	<u>2.7</u>	<u>59.8</u>

482 **Table 3.** Biases, RMS differences<sub>s</sub>, and standard deviations (SD<sub>s</sub>) of the variables between  
483 the RS92 and RS41 radiosondes. The bias is the mean of RS92  $\bar{\text{—}}$  RS41 differences.

484

Variable	Total		MR15-03 (Subarctic – Arctic)		MR15-04 (Subtropics – Tropics)	
	Bias	RMS	Bias	RMS	Bias	RMS
		SD		SD		SD
Temperature (°C)	+0.04	0.17	+0.01	0.15	+0.06	0.19
P <sub>RS92</sub> > 100hPa		0.17		0.15		0.18
Temperature (°C)	−0.01	0.22	−0.10	0.27	+0.05	0.18
P <sub>RS92</sub> < 100hPa		0.22		0.25		0.17
Pressure (hPa)	+0.52	0.67	+0.41	0.58	+0.64	0.76
P <sub>RS92</sub> > 100hPa		0.42		0.40		0.41
Pressure (hPa)	+0.55	0.67	+0.57	0.61	+0.53	0.71
P <sub>RS92</sub> < 100hPa		0.38		0.21		0.47
Relative humidity (%RH)	−0.89	3.14	−0.50	2.14	−1.26	3.86
		3.01		2.08		3.64
Zonal wind speed (m s <sup>−1</sup> )	−0.0017	0.18	+0.0027	0.17	−0.0059	0.18
		0.18		0.17		0.18
Meridional wind speed (m s <sup>−1</sup> )	−0.0051	0.17	+0.0104	0.18	−0.0199	0.16
		0.17		0.18		0.15

485

486

Table 4. Biases and standard deviations of CAPE, CIN and PW between the RS92 and RS41 radiosondes. The bias is the mean of RS92 – RS41 differences. Values in parentheses are the statistics without the two outliers shown in Fig. 7b-c (Flight No. 22 and No. 23).

	<u>MR15-03</u>			<u>MR15-04</u>			<u>MR15-04</u>		
				<u>Daytime</u>			<u>Nighttime</u>		
	<u>RS41</u>	<u>Bias</u>	<u>SD</u>	<u>RS41</u>	<u>Bias</u>	<u>SD</u>	<u>RS41</u>	<u>Bias</u>	<u>SD</u>
	<u>Mean</u>			<u>Mean</u>			<u>Mean</u>		
<u>CAPE</u>	<u>5.3</u>	<u>−0.9</u>	<u>1.8</u>	<u>1196.9</u>	<u>−331.7</u>	<u>614.7</u>	<u>1215.3</u>	<u>111.1</u>	<u>94.8</u>
<u>(J kg<sup>−1</sup>)</u>				<u>(841.5)</u>	<u>(−75.4)</u>	<u>(222.4)</u>			
<u>CIN</u>	<u>0.8</u>	<u>0.8</u>	<u>1.9</u>	<u>9.2</u>	<u>1.1</u>	<u>4.4</u>	<u>16.0</u>	<u>−0.2</u>	<u>1.3</u>
<u>(J kg<sup>−1</sup>)</u>				<u>(10.6)</u>	<u>(1.0)</u>	<u>(5.0)</u>			
<u>PW</u>	<u>13.2</u>	<u>−0.2</u>	<u>0.3</u>	<u>56.3</u>	<u>−0.9</u>	<u>1.1</u>	<u>63.9</u>	<u>0.1</u>	<u>0.5</u>
<u>(mm)</u>				<u>(55.0)</u>	<u>(−0.6)</u>	<u>(1.0)</u>			

494 **Table 45.** Bias correction table of relative humidity that was created by matching the CDFs  
 495 from the RS92 data to the RS41 data (%RH) based on the daytime data obtained during  
 496 the MR15-04 cruise.

	$\leq -80^{\circ}\text{C}$	$-60^{\circ}\text{C}$	$-40^{\circ}\text{C}$	$-20^{\circ}\text{C}$	$0^{\circ}\text{C}$	$\geq 20^{\circ}\text{C}$
2.5 %RH	1.84	0	-0.42	0	0	0
7.5	0.50	2.35	0.50	0.25	0.36	0
12.5	4.12	2.14	3.24	1.15	0.79	0
17.5	6.47	3.13	2.31	1.43	1.00	0
22.5	7.14	3.33	2.86	1.67	1.67	0
27.5	8.93	1.67	4.09	2.50	1.82	0
32.5	8.13	2.50	4.23	3.00	0.88	0
37.5	7.31	2.50	4.33	2.92	4.17	1.67
42.5	6.25	4.06	4.38	2.73	3.75	0.63
47.5	7.50	5.00	2.50	2.78	2.08	4.17
52.5	5.00	5.50	4.17	2.65	1.67	2.14
57.5	0	4.50	5.00	4.09	2.00	1.25
62.5	0	5.00	2.22	5.00	2.76	2.50
67.5	0	5.00	0	4.44	0.80	0.49
72.5	0	0	0	3.27	1.60	1.25
77.5	0	0	0	3.38	1.35	1.44
82.5	0	0	0	2.50	1.45	1.36
87.5	0	0	0	3.00	1.73	0.91
92.5	0	0	0	2.50	0.90	0.56
97.5	0	0	0	0	0	0

498

499



## Figure Captions

**Figure 1.** Positions of the twin-radiosonde launches during the (a) MR15-03 cruise, and (b) MR15-04 cruise. (c) Time-latitude diagram of the launches. Black and red dots represent daytime and nighttime soundings, respectively.

**Figure 2.** Photographs of (upper) the RS92 and RS41 radiosondes directly attached to each other and (lower) a launch on R/V *Mirai*.

**Figure 3.** Vertical profiles of the median (black), 25–75th percentile (green), 10–90th percentile (gray), and mean  $\pm$  standard deviation (cyan) of all differences between the RS92 and RS41 observations (RS92 – RS41) for (a) pressure, (b) geopotential height, (c) relative humidity, (d) temperature, ~~(e) relative humidity~~, ~~(de)~~ zonal wind, and ~~(ef)~~ meridional wind.

**Figure 4.** As in Fig.3a, but for between the RS41 GPS-derived and RS92 pressures (RS92 – RS41).

**Figure 45.** Mean difference in relative humidity between the RS92 and RS41 radiosondes (RS92 – RS41) as a function of the RS41 temperature for relative humidity ranges of 0–20 % (blue), 20–40 % (red), 40–60 % (green), 60–100 % (black), and 0–100 % (gray).

520

521 **Figure 56.** Vertical profiles of the RS41 temperature (red), RS92 temperature (blue), RS41  
522 relative humidity (magenta), and RS92 relative humidity (cyan). (a) Flight No. 29  
523 launched at 1727 UTC on 10 December 2015 in the tropics, and (b) Flight No. 9 launched  
524 at 0530 UTC on 16 September 2015 in the Arctic.

525

526 **Figure 67.** ~~Same as~~ Fig. 56, but for (a) Flight No. 30 launched at 1420 UTC on 11  
527 December 2015, (b) Flight No. 22 launched at 0530 UTC on 1 December 2015, and (c)  
528 Flight No. 23 launched at 0529 UTC on 3 December 2015. All launches in the tropics.

529

530 **Figure 78.** Differences between the RS92 and RS41 radiosonde (RS92 – RS41) results for  
531 daytime (blue) and nighttime (red) flights during the MR15-04 cruise for (a) pressure, (b)  
532 temperature, and (c) relative humidity.

533

534 **Figure 89.** Relative difference between the RS92 and RS41 relative humidity obtained  
535 during the daytime on the MR15-04 cruise (blue dots, %). Relative difference is defined  
536 as the relative humidity difference expressed as a percentage of the RS41 relative  
537 humidity. Green line denotes the median of the relative difference. Lower panel shows an  
538 enlargement of part of the upper panel.

539

**Figure 10.** The ratio of the RS41 to the RS92 PW as a function of solar altitude angle. Blue and red dots represent soundings in the MR15-03 and MR15-04 cruises, respectively.

**Figure 911.** (a) CDFs of relative humidity for the RS92 (bold dashed line) and RS41 (bold solid line) data in the temperature range of  $-90$  to  $-70^{\circ}\text{C}$ . The daytime data obtained during the MR15-04 cruise were used. Thin solid lines illustrate the CDF-matching technique (see text). (b) Bias correction of relative humidity for the same temperature range.

**Figure 4012.** Medians of the relative humidity difference between the RS92 and RS41 radiosondes obtained during the daytime on the MR15-04 cruise. Blue and black lines show the profiles before and after the bias correction of the RS92 data.

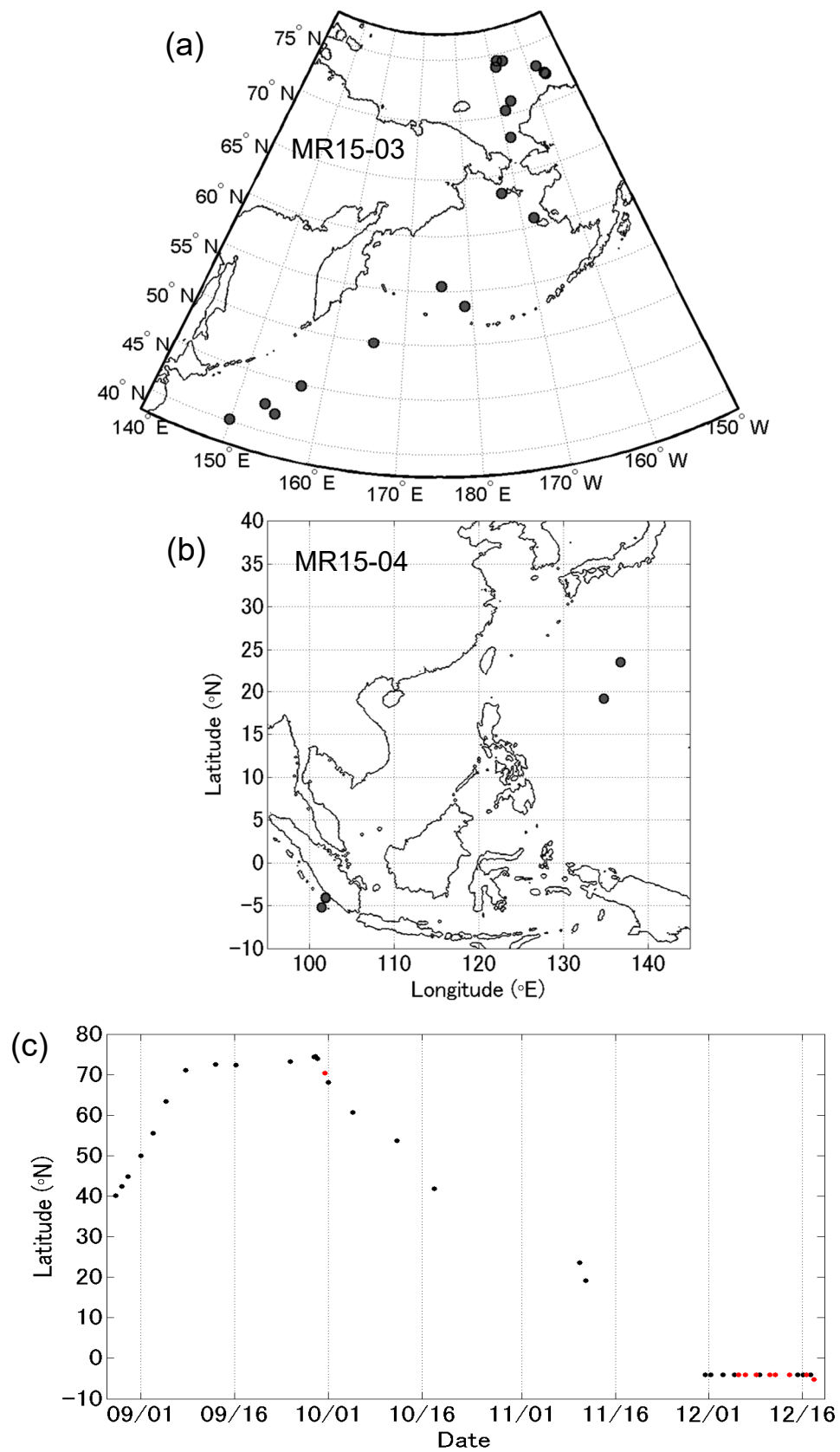


Fig. 1. Positions of the twin-radiosonde launches during the (a) MR15-03 cruise, and (b) MR15-04 cruise. (c) Time-latitude diagram of the launches. Black and red dots represent daytime and nighttime soundings, respectively.



Fig.2. Photographs of (upper) the RS92 and RS41 radiosondes directly attached to each other and (lower) a launch on R/V *Mirai*.

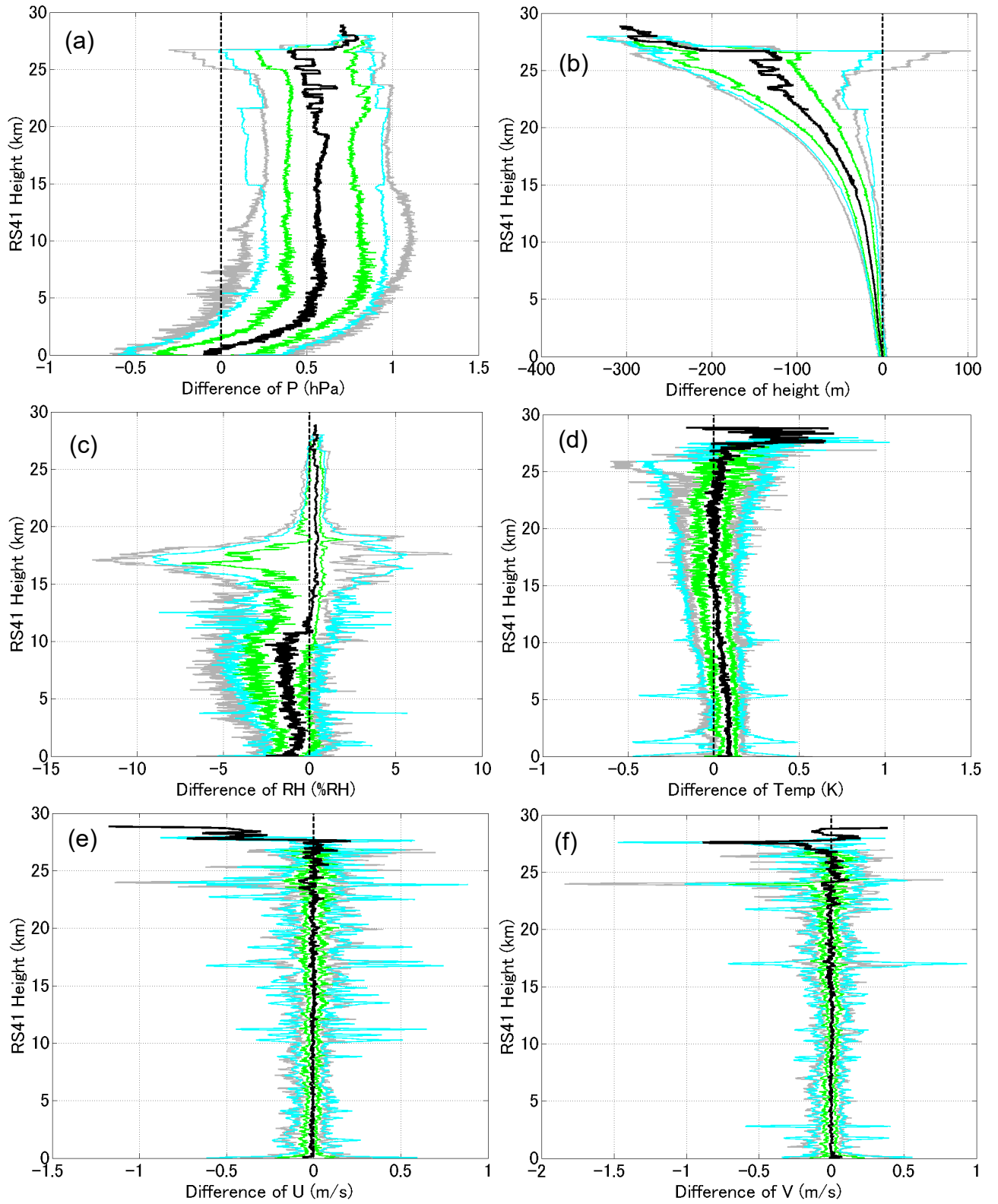


Fig.3. Vertical profiles of the median (black), 25–75th percentile (green), 10–90th percentile (gray), and mean  $\pm$  standard deviation (cyan) of all differences between the RS92 and RS41 observations (RS92 – RS41) for (a) pressure, (b) geopotential height, (c) relative humidity, (d) temperature, (e) zonal wind, and (f) meridional wind.

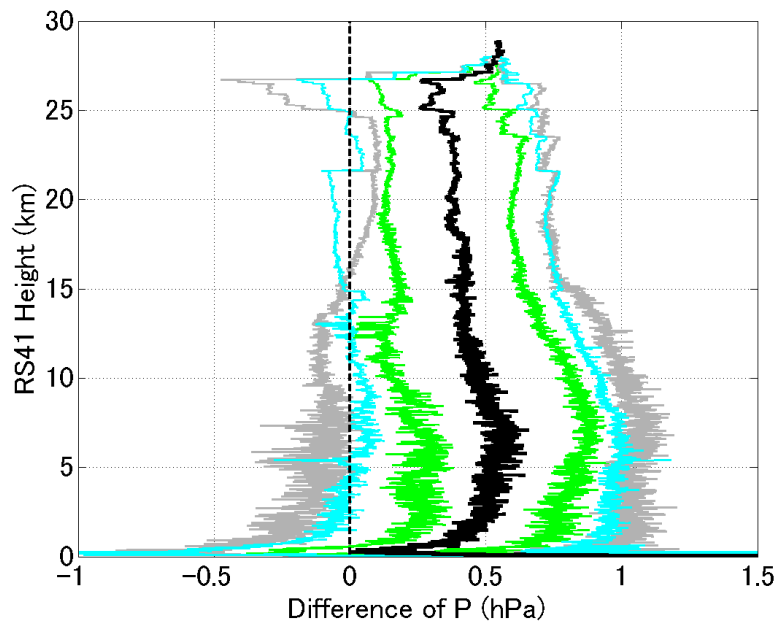


Fig.4. As in Fig.3a, but for between the RS41 GPS-derived and RS92 pressures (RS92 – RS41).

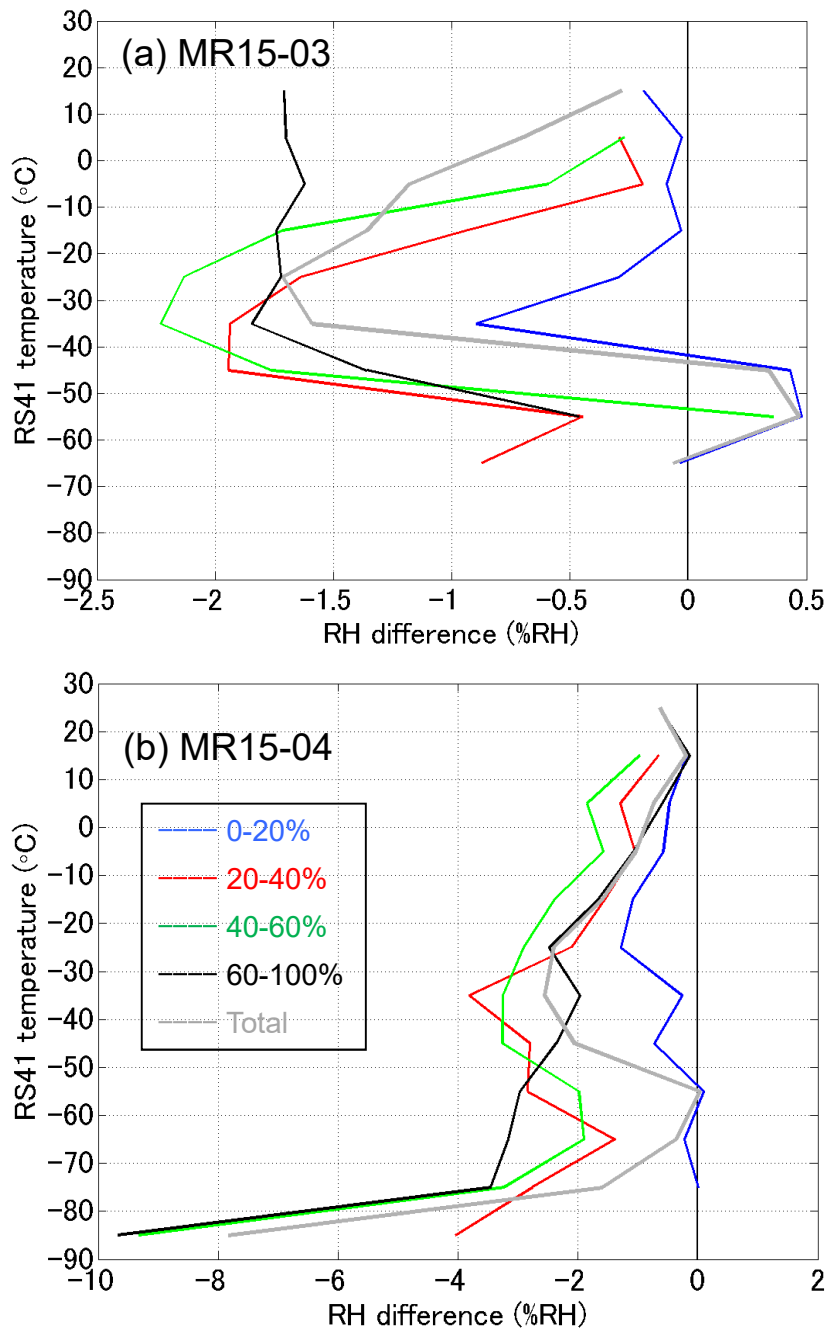


Fig.5. Mean difference in relative humidity between the RS92 and RS41 radiosondes ( $RS92 - RS41$ ) as a function of the RS41 temperature for relative humidity ranges of 0–20 % (blue), 20–40 % (red), 40–60 % (green), 60–100 % (black), and 0–100 % (gray).



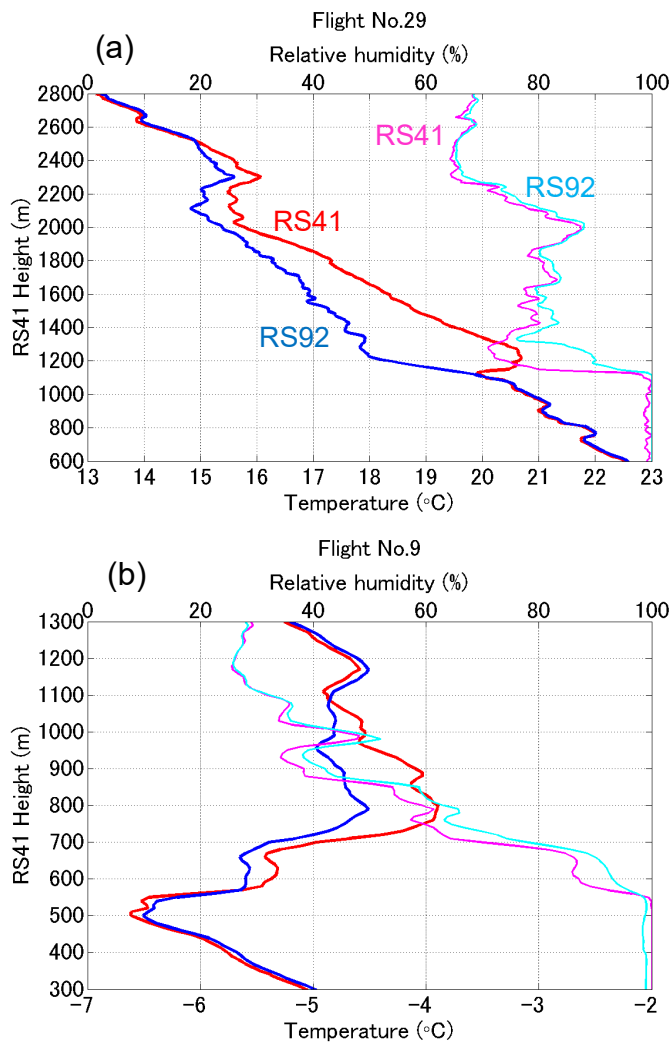


Fig.6. Vertical profiles of the RS41 temperature (red), RS92 temperature (blue), RS41 relative humidity (magenta), and RS92 relative humidity (cyan). (a) Flight No. 29 launched at 1727 UTC on 10 December 2015 in the tropics, and (b) Flight No. 9 launched at 0530 UTC on 16 September 2015 in the Arctic.

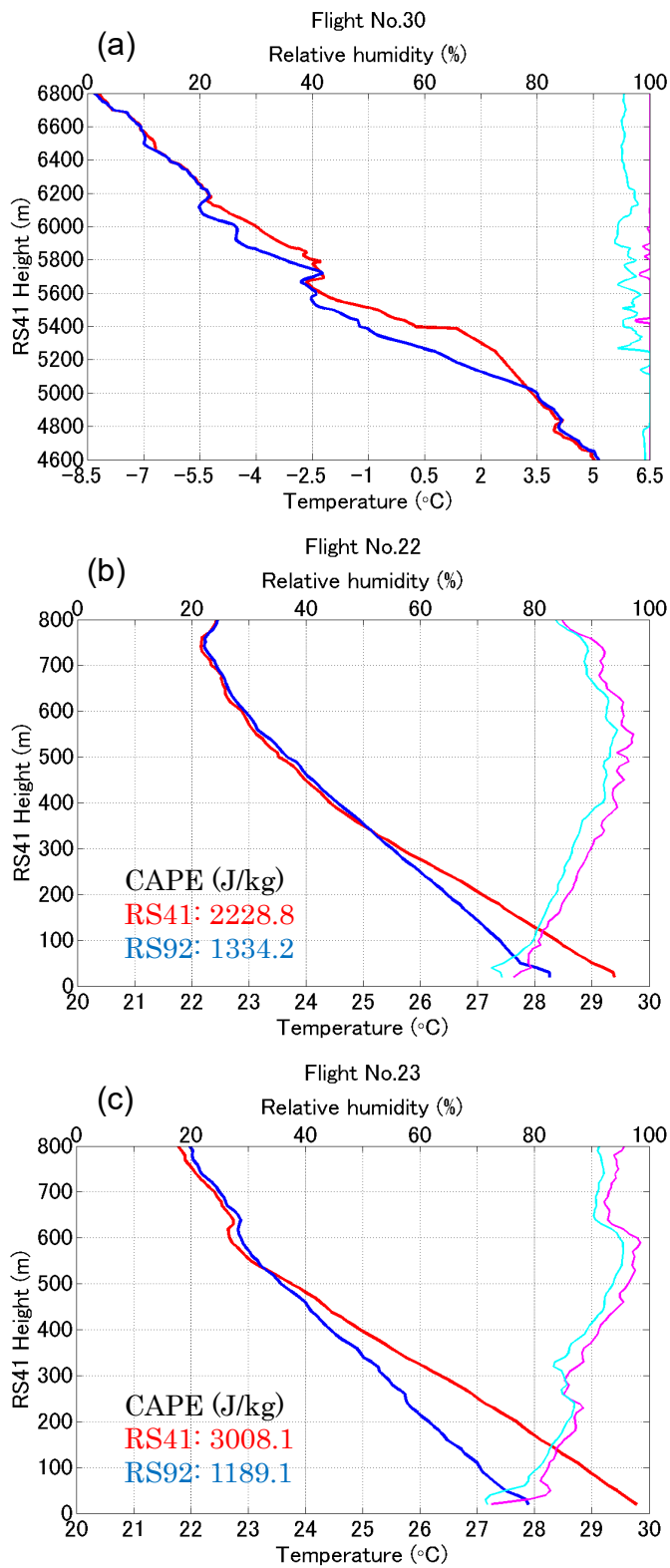


Fig. 7. As in Fig. 6, but for (a) Flight No. 30 launched at 1420 UTC on 11 December 2015, (b) Flight No. 22 launched at 0530 UTC on 1 December 2015, and (c) Flight No. 23 launched at 0529 UTC on 3 December 2015. All launches in the tropics.

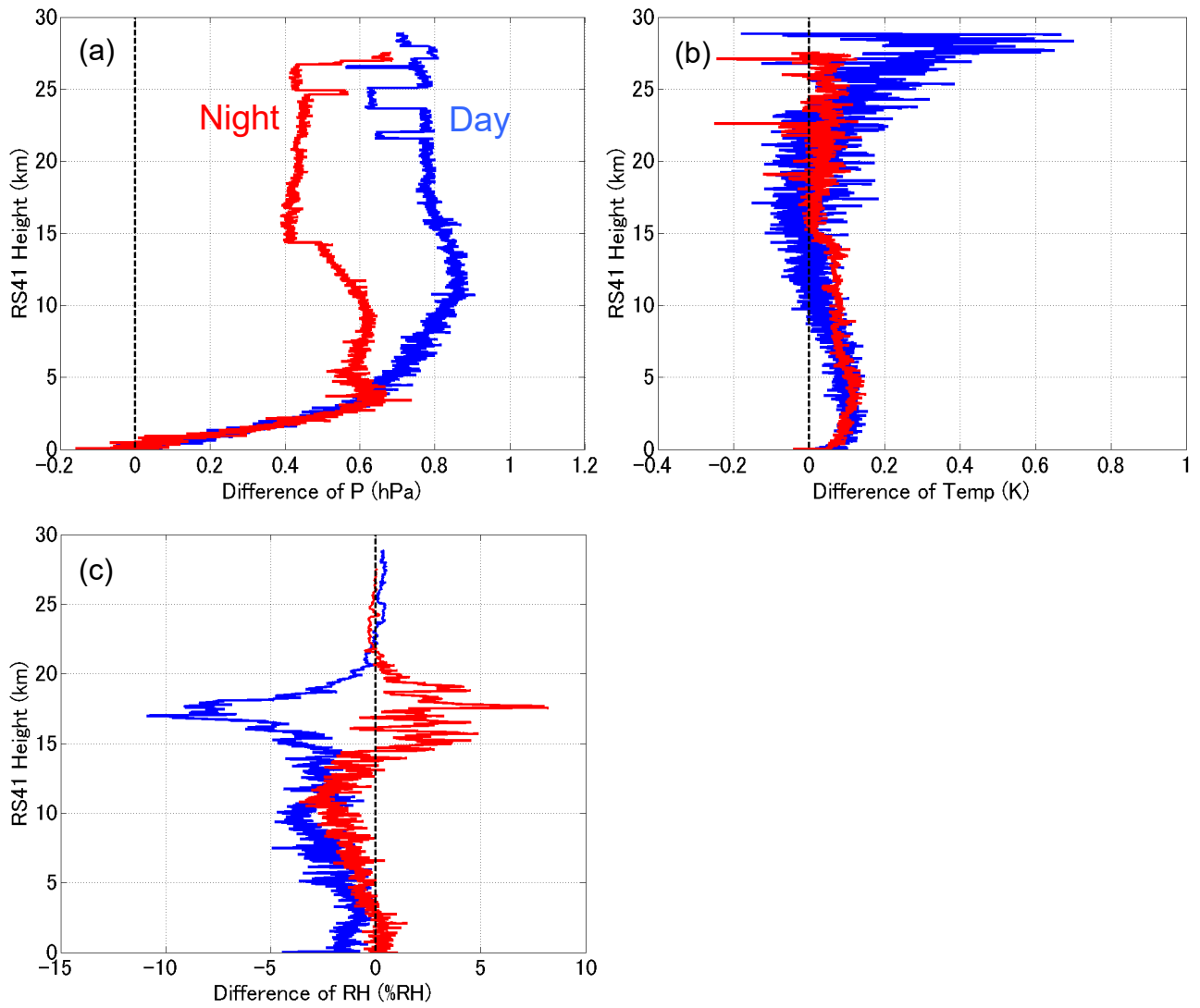


Fig.8. Differences between the RS92 and RS41 radiosonde (RS92 – RS41) results for daytime (blue) and nighttime (red) flights during the MR15-04 cruise for (a) pressure, (b) temperature, and (c) relative humidity.

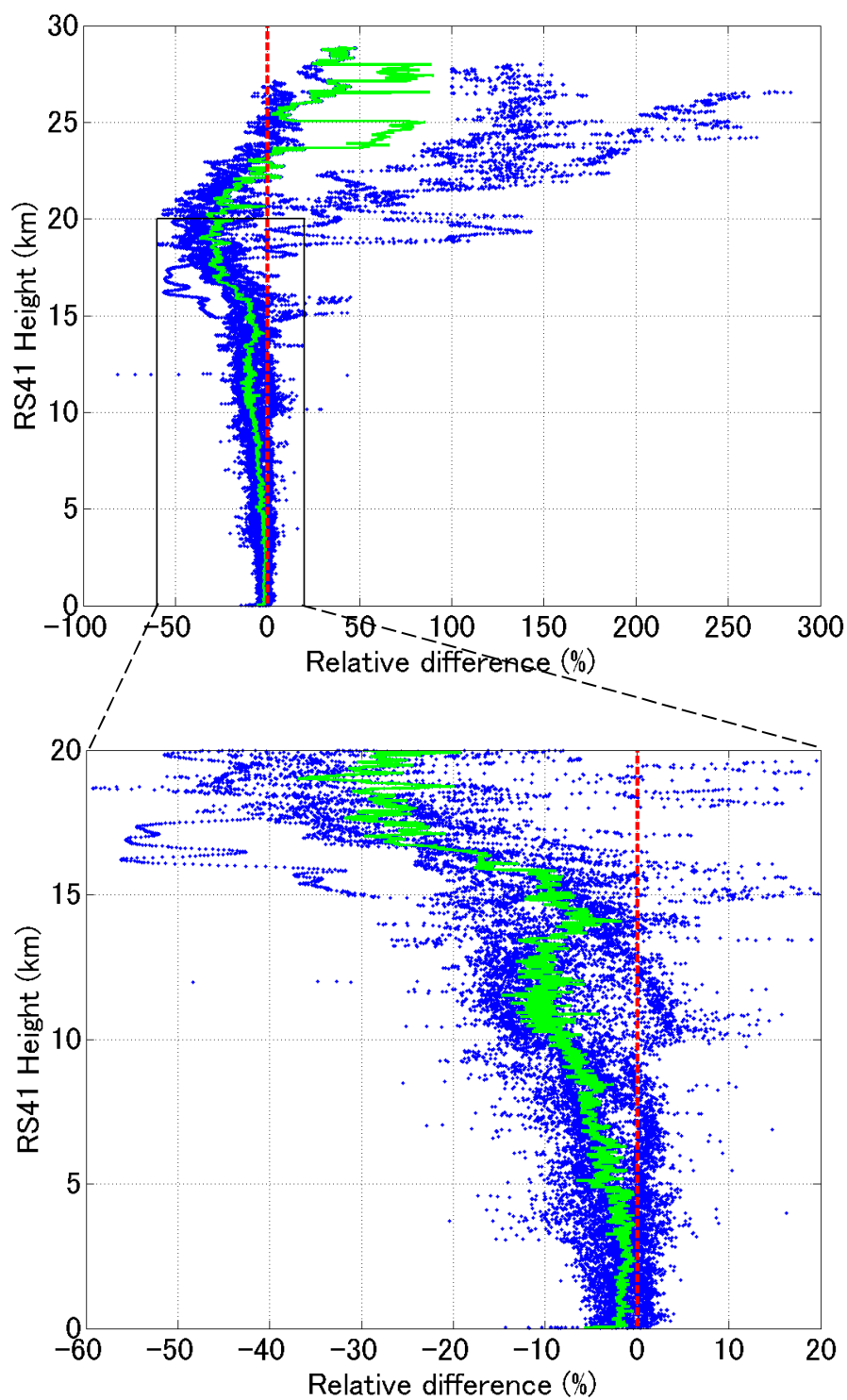


Fig. 9. Relative difference between the RS92 and RS41 relative humidity obtained during the daytime on the MR15-04 cruise (blue dots, %). Relative difference is defined as the relative humidity difference expressed as a percentage of the RS41 relative humidity. Green line denotes the median of the relative difference. Lower panel shows an enlargement of part of the upper panel.

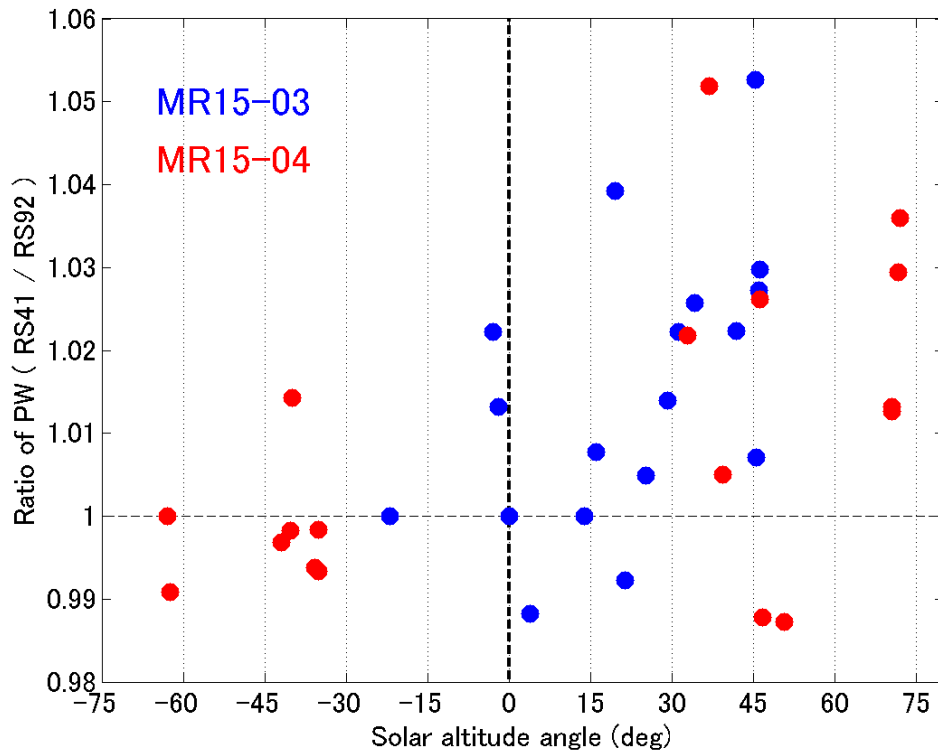


Fig. 10. The ratio of the RS41 to the RS92 PW as a function of solar altitude angle. Blue and red dots represent soundings in the MR15-03 and MR15-04 cruises, respectively.

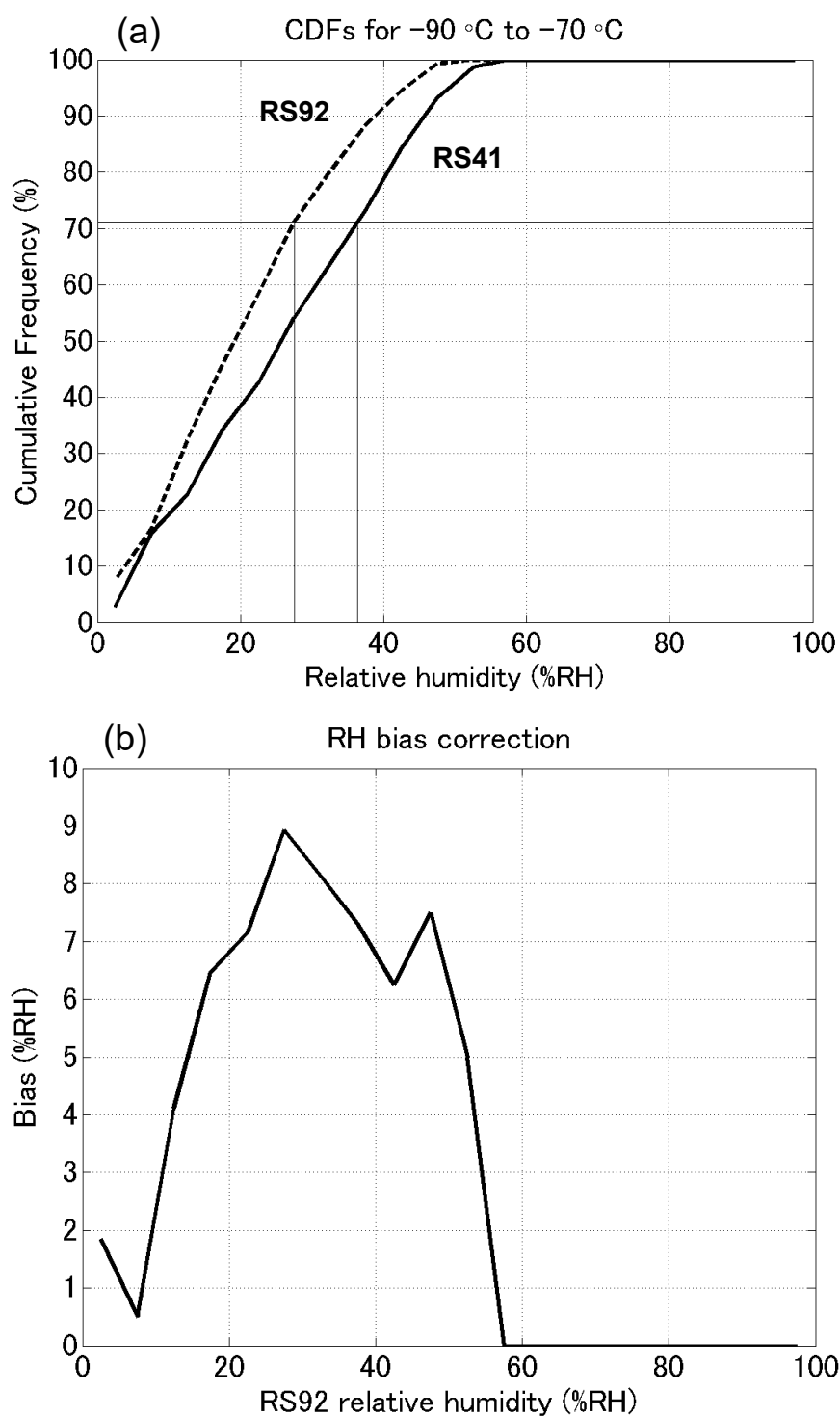


Fig. 11. (a) CDFs of relative humidity for the RS92 (bold dashed line) and RS41 (bold solid line) data in the temperature range of  $-90$  to  $-70^{\circ}\text{C}$ . The daytime data obtained during the MR15-04 cruise were used. Thin solid lines illustrate the CDF-matching technique (see text). (b) Bias correction of relative humidity for the same temperature range.

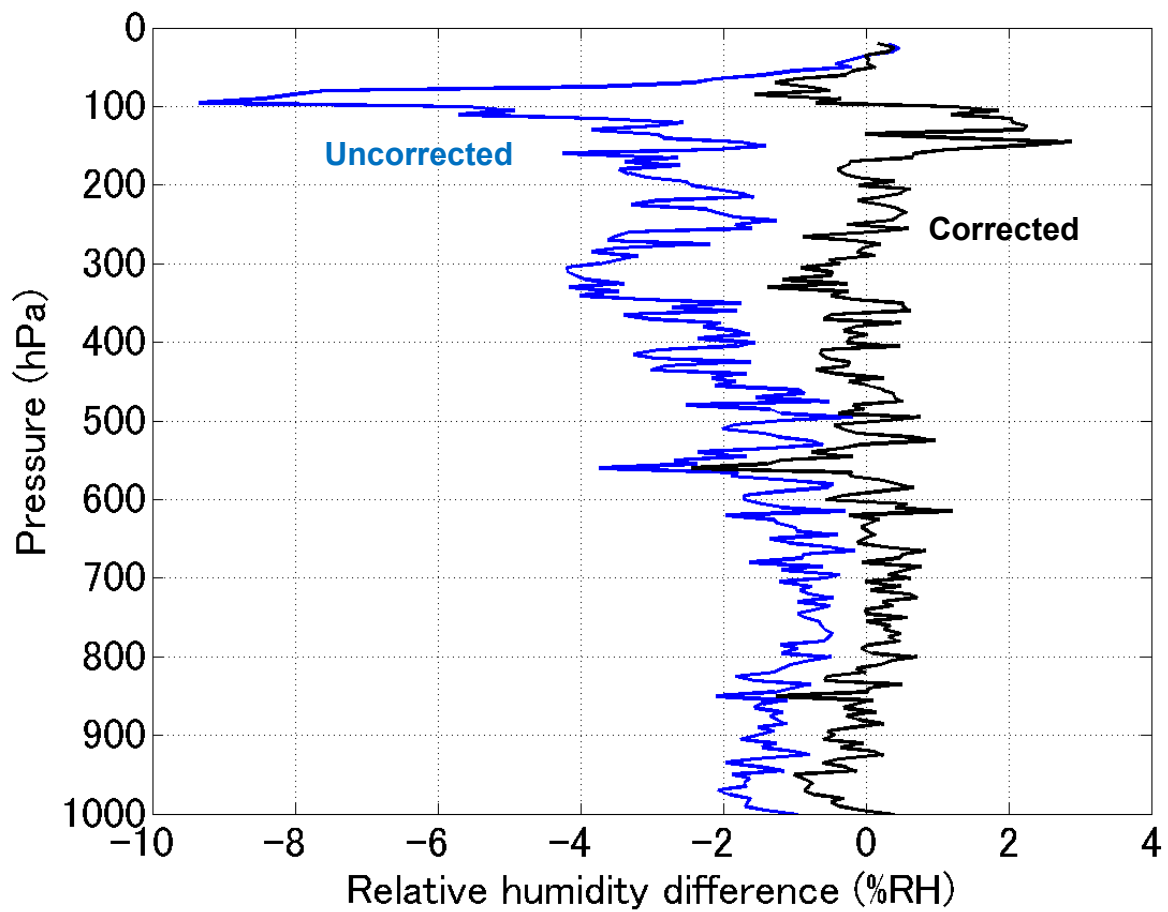


Fig. 12. Medians of the relative humidity difference between the RS92 and RS41 radiosondes obtained during the daytime on the MR15-04 cruise. Blue and black lines show the profiles before and after the bias correction of the RS92 data.